A new function for the yeast trehalose-6P synthase (Tps1) protein, as key pro-survival factor during growth, chronological ageing, and apoptotic stress

Marjorie Petitjean, Marie-Ange Teste, Isabelle Léger-Silvestre, Jean Marie François, Jean-Luc Parrou

Graphical Abstract

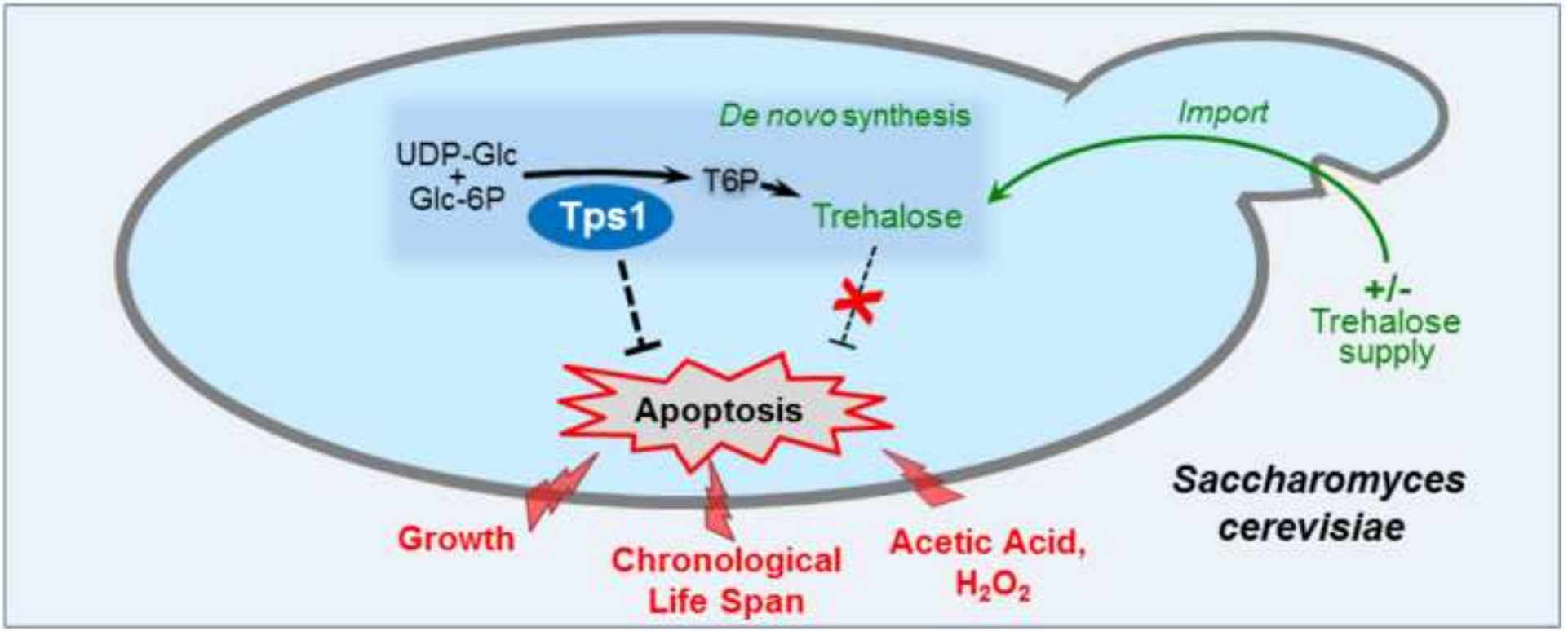

highligts

- The trehalose is not required for yeast longevity and the inhibition of apoptosis
- The Tps1 protein itself protects cells from commitment to apoptosis during growth
- The lack of Tps1p shortens CLS and sensitizes to H_20_2 and AA-triggered apoptosis
- The pro-survival function of Tps1p probably relies on the maintain of ATP charge

A new function for the yeast Trehalose-6P Synthase (Tps1) Protein, as key pro-survival factor during growth, chronological ageing, and apoptotic stress.

Marjorie Petitjean[1,], Marie-Ange Teste[1], Isabelle Léger-Silvestre[2], Jean M. François[1], and Jean-Luc Parrou[1]

[1] LISBP, Université de Toulouse, CNRS, INRA, INSA, Toulouse, France;

[4] Laboratoire de Biologie Moléculaire Eucaryote, CNRS, Université de Toulouse, 118 route de Narbonne, F-31000 Toulouse, France

Contact information : Jean-Luc Parrou, LISBP, INSA, 135 Ave de Rangueil, 31077 Toulouse cedex 04, France, Tel.: 0033 561 55 94 23; Fax: 0033 561 55 94 23; E-mail: jean-luc.parrou@insa-toulouse.fr

ABSTRACT

Looking back to our recent work that challenged the paradigm of trehalose in stress resistance in yeast, our objective was to revisit the role of this disaccharide in chronological life span (CLS), and in the control of apoptosis. Using a catalytically dead variant of the trehalose-6-phosphate synthase (Tps1) protein, (the first enzyme in the trehalose biosynthetic pathway), and by manipulating intracellular trehalose independently of this pathway, we demonstrated that trehalose has no role in CLS or in the inhibition of acetic acid or H_20_2-triggered cell death. We showed instead that, in the absence of any apoptotic stimulus, the Tps1 protein itself was necessary in preventing massive, spontaneous commitment of yeast cells to apoptosis during growth. Without Tps1p, the life span was shortened and cells were sensitized to acetic acid (AA) and H_20_2, whereas the overexpression of the inactive variant of Tps1p almost abolished AA-triggered apoptosis. Genetic interaction analysis of *TPS1* and genes such as *YCA1*, *NUC1* and *AIF1* indicated that these key executioners of cell death partially relayed *tps1*Δ-triggered signalling. Our results suggested that the pro-survival role of Tps1p could be connected with its ability to preserve ATP levels in yeast cells.

Keywords: Anti-apoptotic; Chronological Life Span; Oxidative stress; Acetic Acid; ATP.

1. INTRODUCTION

Apoptosis is described as an evolutionary conserved cell suicide program in response to intracellular or environmental stimuli (Galuzzi, 2014; Falcone & Mazzoni, 2016). The existence of apoptosis in yeast was first reported in 1997, using a *Saccharomyces cerevisiae* strain carrying a mutation on the *CDC48* gene (Madeo et al., 1997). Since that time, studies have assessed the existence of apoptosis in response to various stresses, for example, exposure to acetic acid or to drugs, and also during different physiological scenarios such as chronological aging (CLS) (Fabrizio and Longo, 2003; Ruckenstuhl and Carmona-Gutierrez, 2010; Swinnen et al., 2014). It was indeed shown that chronologically aged yeast cultures die, undergoing an altruistic death program that exhibits typical markers of apoptosis (Allen et al., 2006; Fabrizio et al., 2004; Herker et al., 2004). This active process may allow the most aged or damaged cells to provide nutrients and resources for quiescent cells waiting for growth resumption under more favourable conditions (Allen et al., 2006; Herker et al., 2004). Several orthologues of mammalian apoptotic proteins have been discovered in yeast revealing conserved pathways, which have highlighted the yeast *S. cerevisiae* as a powerful model for apoptosis study in general (Büttner et al., 2006; Carmona-Gutierrez et al., 2010; Greenwood and Ludovico, 2010; Liang et al., 2008; Longo and Fabrizio, 2002; Ludovico et al., 2005; Madeo et al., 2009; 2004; Mazzoni and Falcone, 2008).

The process of cell death and its control remains an intricate molecular puzzle, whose complexity and phenotypic markers are still under debate far beyond the yeast model (Galluzzi et al., 2015; Ludovico et al., 2005; Wanichthanarak et al., 2013). Many subtypes of genetically-controlled cell death processes could be proposed, based on the nature, extent and kinetics of the occurrence of biochemical and morphologic features. As in higher eukaryotic cells, these features include, amongst others, DNA cleavage and chromatin condensation,

phosphatidyl serine (PS) externalization on the outer leaflet of the plasma membrane and also alterations in mitochondrial structure and functions (Braun and Westermann, 2011; Guaragnella et al., 2012; Ludovico et al., 2001a; Mirisola et al., 2014; Wloch-Salamon and Bem, 2013). These mitochondrial dysfunctions are, for example, extensive fragmentation, reactive oxygen species (ROS) accumulation and alteration of membrane potential. Another hallmark of apoptosis is the release of proteins from this compartment, such as the cytochrome c (Ludovico et al., 2002), the NADH dehydrogenase Ndi1p (Cui et al., 2012; Li, 2006), as well as the so-called cell death 'executioners' such as Aif1p and Nuc1p. The cytochrome c was the first mitochondrial protein shown to have an apoptotic function different from its role as an electron carrier in the respiratory chain (Ludovico et al., 2002). The apoptosis-inducing factor (AIF) is a highly conserved protein from yeast to human, which translocates to the nucleus where it participates in chromatinolysis in response to apoptotic stimuli (Wissing et al., 2004). Nuc1p is the yeast homologue of the metazoan endonuclease G (EndoG), a mitochondrial protein with DNase/RNase activity also involved in apoptotic DNA degradation after its mitochondrio-nuclear translocation (Büttner et al., 2007a). Another key executioner of cell death is the type I metacaspase encoded by *YCA1/MCA1* (Madeo et al., 2002; Tsiatsiani et al., 2011; Uren et al., 2000), of which the only substrate described so far is the metabolic enzyme glyceraldehyde-3-phosphate dehydrogenase, which is cleaved under peroxide-induced apoptosis (Silva et al., 2011).

The link between apoptosis and metabolism, that relied notably on antioxidant detoxifying activities and redox homeostasis (Ayer et al., 2014), is being reinforced by studies that unveil functions of 'metabolic' genes in promoting cell death, or conversely exerting pro-survival functions (*e.g. ACH1* (Orlandi et al., 2012), *GPH1* (Favre et al., 2008), *GUP1* (Tulha et al., 2012), *HXK2* (Amigoni et al., 2013), *ISC1* (Almeida et al., 2008), *PGK1* (Mazzoni et al., 2009) or *YDC1* (Aerts et al., 2008)). The accumulation of toxic metabolic intermediates over

time, especially in mitochondria in the absence of specific clearance mechanism, could be one of the causes of the loss of mitochondrial integrity and commitment to cell death (Breitenbach et al., 2014). Other reports strengthened the importance of neutral amino acids which may sustain the vacuolar–mitochondrial cross-talk (Hughes and Gottschling, 2012), and the nucleocytosolic pool of acetyl-CoA that may link histone acetylation and epigenetic changes in chromatin, with autophagy and longevity (Eisenberg et al., 2014; Mirzaei and Longo, 2014).

Other evidence for the link between apoptosis and carbon metabolism rely on trehalose, which may be essential in defining yeast longevity (Kyryakov et al., 2012; Ocampo et al., 2012; Samokhvalov et al., 2004a) and in the inhibition of apoptosis (Kyryakov et al., 2012; Lu et al., 2011). This non-reducing, highly stable disaccharide is especially known as a potent molecular chaperone able to protect cells against a variety of environmental and nutritional stresses (Elbein et al., 2003). It is also known as a reserve carbohydrate present in a large variety of organisms such as fungi, insects and plants (Elbein et al., 2003). In the yeast *S. cerevisiae*, trehalose is synthesized in a two-step reaction. The trehalose-6P synthase (Tps1p) first produces trehalose-6-phosphate (T6P) from glucose-6P and UDP-Glucose. The T6P is then dephosphorylated by a specific trehalose-6P phosphatase (Tps2p), to yield to trehalose. Strains deleted for *TPS1* cannot synthesize trehalose and they exhibit a plethora of phenotypes (François and Parrou, 2001). The most outstanding one is the inability of a *tps1Δ* mutant to grow on rapidly assimilated carbon sources (*e.g.* glucose or fructose), galactose being therefore the usual, permissive carbon source used to cultivate this mutant strain. This inability to grow on glucose or fructose is explained by the rapid drop of ATP and the hyperaccumulation of phosphorylated sugars upon addition of such carbon sources. A consequence of this metabolic defect is the loss of the mutant strain's viability (Blazquez et al., 1993; Gancedo and Flores, 2004; González et al., 1992; Walther et al., 2013). These

results led to the suggestion that Tps1p and/or the trehalose pathway control the entrance of glucose into glycolysis (Thevelein and Hohmann, 1995), but in spite of several models proposed so far (Gancedo and Flores, 2004; Hohmann et al., 1996; van Heerden et al., 2014), the molecular mechanisms underlying this phenotype remain unsolved.

In recent work we revisited the paradigm of trehalose as a stress-protectant in yeast and we showed that the Tps1 protein itself, not trehalose, was the main determinant for stress resistance (Gibney et al., 2015; Petitjean et al., 2015). The objective of the present study is to identify which of the three elements; *i.e.* the Tps1 protein *per se*, T6P or trehalose, actually help maintain yeast longevity and block commitment to apoptotic cell death in a wild type strain. To this end, we used the same strategy as in Petitjean et al. (Petitjean et al., 2015). It consisted of the expression of a catalytically inactive variant of Tps1p, encoded by *tps1-156*, which was unable to synthesize trehalose. In parallel, we manipulated trehalose levels by the use of the laboratory CEN.PK strain (Van Dijken et al., 2000), which enabled the uptake of the exogenous disaccharide by the constitutively expressed Agt1 transporter (Plourde-Owobi et al., 1999). Our results proved that trehalose does not protect cells from entering apoptosis, a role that is fully endorsed by the Tps1 protein itself, independently of its known catalytic function. We also showed that a basal level of the Tps1 protein is necessary, and sufficient, to protect cells from premature cell death during growth on any carbon source, to maintain chronological life span and to constrain the apoptotic response to different stimuli. Altogether, these results led to the proposition that the Tps1 protein is a major pro-survival factor in the yeast *Saccharomyces cerevisiae*.

2. MATERIAL and METHODS

2.1. Strains constructions and validation

The *S. cerevisiae* strains used in this study were derived from the CEN.PK113-7D, a prototrophic *MAL* constitutive strain (Van Dijken et al., 2000). Strains *tps1*Δ (JF1476) and *tps2*Δ (JF248) were previously described in Guillou et al. (2004) and Petitjean et al. (2015), respectively. Construction of the *tps1-156* allele leading to the catalytically dead Tps1^{D156G} variant of the Tps1 protein, has been described in our recent paper (Petitjean et al., 2015).

All other knockout mutants presented in this work were constructed using the Yeast Knockout strain Collection from Open Biosystems (#YSC1053), available in the BY strain background. Using recommended primers for locus amplification and validation, each knockout of interest was PCR amplified and both the control (*TPS1*) and *tps1*Δ strains were transformed by these PCR products, leading either to single or to double mutants with *tps1*Δ, in the CEN.PK strain background. Overexpression of *TPS1* and *tps1-156* alleles was carried out using the pGP564 2µ plasmid (Jones et al., 2008), with coding sequences under the native *TPS1* promoter (pMP26 and pMP27, respectively). As in Petitjean et al. (2015), the strain that overexpresses the *tps1-156* allele was validated, to demonstrate that this allele fails to make trehalose even when expressed at high-copy (data not shown). First, Western blotting against Tps1 validated the overexpression of the protein. Second, this strain exhibited no measurable trehalose-6P synthase activity *in vitro*. Third, *in vivo*, trehalose-6P was below the detection level upon glucose addition to trehalose grown cells, even in the *tps2*Δ background. As a final proof for trehalose-6P synthase deficiency *in vivo*, we validated the inability of cells to produce trehalose under heat shock to 42 °C.

2.2. Culture conditions

Unless otherwise stated, yeast cells were cultivated in YN synthetic medium (yeast nitrogen base without amino acids and ammonium at 1.7 g/L (Difco)), supplemented with ammonium

sulfate at 5 g/L, complete drop-out when required (MP-Biomedicals CSM) and 2% (w/v) galactose (YN Gal medium) or 2% galactose plus 1% trehalose (YN GalTre medium). The medium was buffered at pH 4.8 by the addition of 14.3 g of succinic acid liter^{-1} and 6 g of NaOH liter^{-1}. This buffered pH allowed us to maintain optimal growth, (exponential until A_{600} 3-4, as judged from exponential regression analysis of the growth curves, (see a representative experiment in Fig S1, and Parrou et al. (1999)), even when the cultures were conducted in shake flasks (0.5-liter Erlenmeyer flasks with a working volume of 100 mL, at 30 °C and 200 rpm on a rotary shaker).

2.3. Yeast Chronological Life Span assay

Yeast Chronological Life Span (CLS) was assayed following a standard procedure (Longo and Fabrizio, 2012). Overnight cultures from a single colony were diluted (1:200) into 10 mL fresh YN Gal medium, grown to exponential phase and further diluted to A_{600} 0.5–0.7 in 100 mL YN Gal or YN GalTre medium. These cultures were then incubated at 30 °C on a rotary shaker (200 rpm) for several weeks, taking as reference time the moment when the culture reached A_{600} 1.0 (exponential growth).

2.4. Stress exposure

Stress exposure was carried out on exponentially growing cells (A_{600} 0.5–0.7) cultivated on YN Gal or YN GalTre medium at 30 °C, after inoculation with a cell density of A_{600} 0.025. For the oxidative stress, the culture was directly treated by addition of hydrogen peroxide 0.5 M (H_2O_2, sigma, 7722-84-1) to a final concentration of 1 mM, 5 mM or 10 mM. Acetic acid exposure was carried out according to previously described procedures (Giannattasio et al., 2005; Ludovico et al., 2001a). Exponentially growing cells were transferred in a YN Gal adjusted to pH 3,0 with HCl, and containing or not (control) acetic acid 40 mM, 80 mM and 120 mM (adapted from Ludovico et al. (2001b)). Incubation in the presence of the chemicals was performed at 30 °C, up to 4 h.

2.5. Other analytical procedures

Cell sampling and metabolites extraction were carried out as previously described in Walther et al. (2010). The ATP content was determined enzymatically by the production of NADH as follows. The reaction was carried out at 30 °C in Tris-HCl buffer with NAD+ 0.4 mM, glucose 1 mM, 4.5 U/ml Glucose-6-phosphate dehydrogenase and 1.5 U/ml hexokinase. NADH production was then assessed at 340 nm (spectrophotometer Agilent G1103A). Trehalose measurement was done according to Parrou and François (1997).

2.6. General settings for flow cytometric analysis

Flow cytometric analyses were carried out on the Attune® Acoustic Focusing Cytometer (Life Technologies, Inc.). Cytometer acquisition was run at 100 µL/min to ensure high specificity, on a total number of 100,000 events/run. For all the assays described below, the source of excitation was the 488-nm laser (blue). Voltage calibration of the cytometer was always performed by using the unstained, control sample of the WT strain and further checked on the *tps1*Δ strain. Routinely applied voltages were 2,000 mV for the forward scatter (FSC) and 2,600 mV for the side scatter (SSC). To get auto-fluorescence signal below the 10^3-threshold, calibration settings of the emission filters were 1,200 mV for the 525-nm filter (BL-1), 1,900 mV for the 575-nm filter (BL-2) and 2,100 mV for the 670-nm filter (BL-3). Besides the *TPS1* and *tps1*Δ control strains, unstained samples from strains of interest were analyzed to ensure that these calibration settings for the side scatter-forward scatter plot and for the auto-fluorescence could apply.

2.7. Cell viability

The relative percentage of living and non-viable cells in the population was determined using the Guava® ViaCount® reagent (4000-0040, purchased from Millipore). Flow cytometric analysis was performed using the 525-nm emission filter (BL-1) for the nuclear dye that stains only nucleated cells, and the 670-nm filter (BL-3) for the viability dye that brightly stains

dying cells. Full procedure for sample handling and data analysis has been thoroughly described in Petitjean et al. (2015).

2.8. Mitochondrial membrane potential

Mitochondrial membrane potential was measured using the fluorescent, potential-sensitive dye Rhodamine 123 (Rh123, Molecular Probes #R-302), following an assay adapted from Ludovico et al. (2001a). Briefly, cells were diluted at a concentration of 10^6 cells/ml in PBS (pH 7,0) and independently stained with Rh123 50 nM for 10 min at room temperature, in the dark, and with 1µg/ml of Propidium Iodide (PI, #V13241, Life Technologies). Analysis was performed using the 525-nm emission filter (BL-1), concluding for hyperpolarization of mitochondria when the cells presented a fluorescence signal above the 10^4-treshold, while cells with depolarized mitochondria led to a signal below 10^2 AU (AU, Arbitrary Units of fluorescence), indistinguishable from the autofluorescence. To determine the mitochondrial potential only on viable and apoptotic cells, PI-positive cells were excluded from the measurement (Ludovico et al., 2001a). Hyperpolarization and depolarization profiles were confirmed on WT cells treated by nigericin and FCCP, respectively, according to Ludovico et al., (2001a) (Fig. S2).

2.9. DNA fragmentation

DNA fragmentation was assayed using the APO-BrdU™ TUNEL assay (#A35125, Life technologies) according to (Madeo, 1999) recommendations. For fixation, cells were suspended at $2x10^6$ cells/ml in 500 µL PBS. This cell suspension was mixed with 5 mL of 3.7% formaldehyde and incubated on ice for 15 min. After centrifugation (500 g, 5 min), cells were washed two times with PBS, suspended in 5 ml PBS and then added to 5 ml ice-cold ethanol 70% for overnight incubation at -20 °C. For strand breaks labelling, ethanol-fixed cells were rinsed in the provided wash-buffer and incubated in extemporaneously prepared DNA-labelling solution, at 37 °C with mild shaking on a steering wheel. After 4 hours, cells

were washed and incubated for 30 min at room temperature in the antibody staining solution, then finally stained for another 30 min in the PI staining buffer. Samples were directly analyzed by flow cytometry using the 525-nm (BL-1) and 575-nm (BL-2) emission filters. Negative cells to staining overlaid cells auto-fluorescence (signal between 10^2 and 10^3 AU), while positive cells positioned between 10^4 and 10^5 AU on the BL-1 axis. For each independent experiment, the positive and negative controls provided in the kit were performed and analyzed in parallel.

2.10. Caspase activity

Caspase quantification was performed according to Madeo et al. (2002) using the CaspACE™ assay (#7461, Promega). A total of $5x10^6$ yeast cells were harvested, washed once in PBS, and incubated for 20 min at 30 °C with 200 µl of staining solution containing the FITC-VAD-FMK substrate. Cells were then washed in PBS and suspended in 200 µl PBS for flow cytometry analysis using the 525-nm emission filter (BL-1). Quantification was performed on the FSC *vs.* BL-1 dot blot, where positive cells for caspase activity positioned between 10^3 and 10^5 AU on the BL-1 axis.

2.11. ROS accumulation

ROS detection *in situ* was performed using the the CellROX® Green Reagent (Life technologies, #C10444) according to manufacturer recommendations. Briefly, cells were concentrated at $2x10^7$ cells/ml and the CellROX® Reagent was added at 5 µM final concentration. After 30 minutes at 37 °C, cells were washed three times with PBS. Sample analysis by flow cytometry was performed using the 525-nm emission filter (BL-1). Quantification was performed on the FSC *vs.* BL-1 dot blot, where fluorescence signal above the 10^3-threshold on the BL-1 axis indicated positive cells for ROS accumulation.

2.12. Membrane modifications

Externalization of phosphatidyl serine on the outer leaflet of the plasma membrane was assayed using the Dead Cell Apoptosis Kit with Annexin V Alexa Fluor® 488 & Propidium Iodide (#V13241, Life Technologies). For samples preparation, cells were washed in cold PBS and diluted in the 1X annexin-binding buffer at a final concentration of $2x10^6$ cells/ml. For each 100 µl aliquot, 10 µl of conjugated Annexin V solution and 1 µl of 100 µg/ml PI solution were added, and cells were incubated for 15 minutes at room temperature. After this incubation period, 400 µl of 1X annexin-binding buffer was added and samples were analyzed by flow cytometry using the 525-nm (Annexin V) and 575-nm (PI) emission filters. When analyzing the 525-nm *vs.* 575-nm scatter plot, fluorescence below 10^3 AU for both axes indicated viable cells. Cells with fluorescence signal beyond 10^3 AU on the Annexin V axis with low PI signal were considered as primary apoptotic cells. Conversely, cells positioning beyond 10^3 AU on the PI axis with low annexin V signal were considered as necrotic. Finally, cells positioning beyond 10^3 AU on both axes were considered as secondary apoptotic cells.

2.13. Visualization of mitochondria by confocal microscopy

To visualize mitochondrial network organization, *TPS1* and *tps1Δ* cells were transformed with a pYX222-mtDsRed plasmid (Campbell Gourlay's plasmid, kind gift from Dr Paula Ludovico, Life and Health Sciences Research Institute (ICVS), Braga, Portugal). Confocal microscopy was performed with a confocal disk system (Revolution Nipkow; Andor Technology) installed on an inverted microscope (IX-81; Olympus) featuring a CSU22 confocal spinning disk unit (Yokogawa Corporation of America) and an EM charge-coupled device (CCD) camera (DU 888; Andor Technology). This system was controlled using the mode "Revolution FAST" of Andor Revolution IQ1 software (Andor Technology). Images were acquired using a 100× objective lens (Plan-Apochromat, 1.4 NA, oil immersion; Olympus). Single laser lines used for excitation were Diode Pumped Solid State Lasers

(DPSSL) exciting DsRed at 561 nm (50 mW; Cobolt Jive). A bandpass emission filter (FF01-512/630-25, Semrock) allowed collection of the red fluorescence. 250-nm z steps were used. Exposure time was 2 ms.

2.14. Statistical analysis

Statistical analyses, that is, One-Way and Two-Way ANOVA tests, were conducted by using the PRISM software, and p-value below 0.01 as statistically significant level. When it appeared necessary to sustain ambiguous conclusions, p-value results have been shown, as star(s) that sit on top of brackets, on Excel graphs. The Hierarchical Ascendant Classification (HAC) of single and double mutants was carried out using the STATGRAPHICS Centurion 16 software. This analysis was conducted according to the Ward method, with default parameters (standardization of the data and squared Euclidean distances), by using the whole set of quantitative data available for these strains (*i.e.* viability and all apoptotic markers data).

3. RESULTS

3.1. The deletion of *TPS1* impacts cell growth and viability.

Among the numerous phenotypes of *TPS1* loss-of-function, we particularly observed that *tps1*Δ cells growing on any permissive carbon sources had a very low cell viability (Petitjean et al., 2015). We also noticed that the growth rate on galactose of this mutant was not only slower than that of the wild type, but highly variable between experiments, and that this growth rate correlated with cell viability of the population (Fig. S1.B). Based on the general growth kinetics principle that at any time during growth cells can either divide, or die (Fig. S1.C1), we found that viable *tps1*Δ cells grow and divide as fast as WT cells, with a mean intrinsic growth rate of about 0.34 h^{-1} (Fig. S1.C4). We therefore concluded that this apparent low growth rate of the *tps1*Δ mutant resulted from massive and premature cell death within the population. We have already shown that this lethality could not be prevented by preloading *tps1*Δ cells with trehalose (Petitjean et al., 2015). Conversely, this cell death was not observed in *tps1-156* cells expressing the catalytically inactive $Tps1^{D156G}$ variant, indicating a crucial role of the Tps1 protein *per se* in cell viability during growth.

3.2. The Tps1 protein protects growing cells from spontaneous apoptotic cell death.

This unexpected commitment to cell death of a *tps1* null mutant prompted us to characterize this death process by analyzing specific morphological and biochemical markers (Carmona-Gutierrez et al., 2010). As is shown in Figure 1, almost 40% of *tps1Δ* cells in the exponential phase of growth on galactose presented phosphatidyl serine externalization (~5% for the WT strain) and 20% of them exhibited caspase activity and DNA fragmentation (less than 5% for the WT). Chromatin condensation was also investigated by DAPI staining and microscopy, but no significant difference was observed between WT and *tps1*Δ nuclei. In contrast, the *tps1*Δ mutant showed a clear mitochondrial DNA fragmentation and altered mitochondrial

function, as 80% of these cells presented hyperpolarization of mitochondria (see also Fig. S2) and more than 40% exhibited increased ROS levels (less than 10% for the WT). We finally looked at the structure of the mitochondrial network by using the mtDsRed mitochondrial marker. While the WT showed a clear tubular structure, we observed a total disruption of the mitochondrial network in the *tps1*Δ mutant, with unambiguous thread-grain transition (Fig. 1B). Considering these characteristics, we concluded that the *tps1*Δ mutant strain committed to an apoptotic cell death process.

Very interestingly, these apoptotic traits were abolished in the *tps1-156* strain that expresses a catalytically dead variant of Tps1p. As for the WT strain however, the basal, yet statistically significant 10% loss of viability during growth on galactose, which correlated with 5-10% positive cells for apoptotic markers, was still observed in this *tps1-156* strain. Further, this basal loss of viability was not overriden by the overexpression of Tps1p, either from *tps1-156* or *TPS1* alleles on a 2µ plasmid. These apoptotic markers were similarly observed in cells cultivated on other carbon sources (data not shown). These included galactose supplemented with trehalose, also a mix of glycerol-lactate-ethanol used as a pure respiratory carbon source medium, or trehalose alone, a condition that perfectly mimics glucose-limited oxidative growth in chemostat (Jules et al., 2005, 2004). Taken together, these results showed that the apoptotic cell death occurring in the *tps1*Δ mutant during growth was due to the lack of the Tps1 protein itself, not to trehalose that had no role in protecting cells against this process.

3.3. The Tps1 protein, not trehalose, warrants a normal chronological lifespan.

It has been emphasized that trehalose plays an essential role in the extension of yeast chronological life span (Kyryakov et al., 2012; Palabiyik and Jafari Ghods, 2015; Samokhvalov et al., 2004a, 2004b; Trevisol et al., 2011). The above results prompted us to revisit this conclusion by determining viability and evolution of apoptotic markers during long-term growth of the *tps1-156* strain, which expresses the Tps1 protein but is unable to

synthesize trehalose. As can be seen in Figure 2A, the viability of the *tps1*Δ mutant dropped by *approx.* 1,000-fold during a 4-weeks' incubation, whereas that of WT and *tps1-156* strains remained high with a 30% survival rate at the end of the assay. By cultivating these strains on YN GalTre medium, (which leads to the huge accumulation of trehalose in these cells), cell death kinetics were not altered in any of the three strains (only *tps1*Δ is shown). However, by overexpressing *TPS1,* or by deleting *TPS2,* survival rates were slightly lowered after 4 weeks (15% for these two strains *versus* 30% for the WT strain). This slight drop of viability occurred independently of the presence of trehalose in the culture medium (data not shown). These results suggested that T6P, whose levels were significantly higher in these two mutants as compared to the WT (data not shown but see Walther et al. (2013)), had a negative effect on yeast CLS. From these data, we also concluded that the Tps1 protein, and not trehalose, the end product of Tps1p metabolic pathway in yeast, is needed for normal survival during chronological ageing.

Figure 2 also reports the evolution of apoptotic markers during ageing. The most singular phenotype for the *tps1*Δ strain, whose mitochondria were hyper-polarized during the exponential growth (A_{600}~1), was the massive de-energization of mitochondria, which started even before the diauxic shift (data not shown) and persisted all along the assay as seen for days 9 and 22. Overall, it could be seen that the percentage of positive cells for ROS accumulation, AnV staining and caspase activity, steadily increased during the assay in all strains (Fig. 2B-E), with no statistically significant difference between *tps1-156* and overexpressing strains as compared to the WT strain. Also, we were not able to measure any significant difference for these strains in the presence of trehalose (YN Gal *versus* YN GalTre culture media, data not shown). These data further discarded any role of trehalose in preventing commitment to apoptosis.

3.4. The Tps1 protein constrains both acetic acid and H_2O_2-triggered apoptotic responses

The unpredicted apoptotic state of *tps1*Δ cells growing in the absence of any stimulus, led us to investigate the behavior of this strain when challenged to various exogenous apoptotic stimuli (Fig. 3). To visualize the sole effect of stress exposure, we considered the variable, initial apoptotic states of the different strains in the exponential phase. We then calculated the changes in the percentage of viable cells and positive cells for apoptotic markers, that is, the difference between the values measured after exposure to the stress of interest for 4 hours, and the values measured during the exponential growth. As is shown in Figure 3A, the deletion of *TPS1* greatly sensitized yeast cells to the exposure to 40–120 mM acetic acid (AA) and to 1–10 mM peroxide (H_2O_2), while the WT and *tps1-156* strains showed similar dose-response patterns to these chemicals. Furthermore, we found that preloading the cells with trehalose had no protective effect against these apoptotic stimuli (not shown). These results indicated that the presence of the sole Tps1 protein was sufficient to guarantee WT phenotypes. It is worth noting that, as compared to other yeast strains reported in published data, the lower sensitivity to chemicals of the WT strain used in this study may be explained by the use of the CEN.PK strain background, which was already found to be more resistant than the BY strain to heat shock, oxidative stress and dehydration (see Fig. S3 and Petitjean et al. (2015)).

A singularity of *tps1*Δ in response to H_2O_2 treatment was the significant increase in the proportion of cells presenting AnV/PI co-staining and PI-only staining (*approx*. 60% and 10%, respectively, under 10 mM H_2O_2, Fig. 3D). This indicated that exposure to this chemical strongly damaged cells that committed to secondary apoptosis, and necrosis for a few of them. With regard to acetic acid exposure; the lower dose of 40 mM AA led to a 40% drop of viability for the mutant, as compared to 8% for the WT, which was accompanied by a marked rise in positive cells for ROS accumulation and PS externalization. However, the *tps1*Δ strain

exhibited moderate changes in the number of positive cells with alterations of mitochondrial polarization, caspase activity and DNA fragmentation, even when challenged with increasing AA concentration. This counter-intuitive result could be explained by the strong apoptotic features of the *tps1*Δ strain that are observed already in exponential phase cells, such as hyperpolarized mitochondria, which may preclude further extensive changes of these parameters under stress.

Remarkably, increasing the amount of the $Tps1^{D156G}$ protein by overexpressing the *tps1-156* allele very nearly removed the sensitization of yeast cells to AA exposure. It was illustrated by a marginal drop of viability and almost no increase in positive cells for the different apoptotic markers, even at the higher AA concentration. This effect was not observed in yeast cells overexpressing the wild type *TPS1* allele, indicating that, as for CLS assay, the Tps1p-dependant hyperaccumulation of T6P is somewhat toxic and antagonistic to the positive effect of the sole Tps1 protein that should have been expected. Curiously, contrary to AA exposure, the overexpression of the *tps1-156* allele did not provide any benefits to *tps1*Δ cells exposed to peroxide. This suggested that the molecular targets of Tps1p, that help constraining these various apoptotic responses, are multiple and partly specific to the pathway that is triggered.

3.5. Molecular machinery involved in *tps1Δ*-triggered cell death execution during growth and under exposure to extrinsic stimuli

The commitment to apoptosis of *tps1*Δ led us to investigate the genetic interaction between *TPS1* and a few genes coding for effectors of apoptosis, namely *AIF1*, *NUC1*, *YCA1* and *NDI1*. The whole set of quantitative data on viability and apoptotic markers, (which were determined in each single and double mutant strain during exponential growth), allowed us to conduct a cluster analysis (HAC) that classified the strains into two categories (Fig. 4). One class contained all the strains bearing the *tps1Δ* mutation. The second one gathered the WT and *tps1-156* strains together with all single mutants. This classification was not surprising,

since, in agreement with literature, none of the single disruptants in the WT's cluster exhibited apoptotic features during growth. A notable exception was the *nuc1Δ* strain that classified in this WT's cluster, and did not exhibit any apoptotic feature, while it has been shown to exhibit apoptotic cell death during the exponential growth on a glucose synthetic medium (Büttner et al., 2007b).

The cluster of all double disruptants with *tps1Δ* indicated that none of these deletions enabled to fully recover WT profile. However, more detailed analysis of the different patterns showed that three out of the four mutations brought partial rescue of *tps1Δ* phenotypes, that is, *aif1Δ, nuc1Δ* and *yca1Δ.* Deletion of *NUC1* and *AIF1* in the *tps1Δ* background similarly improved viability and diminished the percentage of positive cells for most of the parameters (Fig. 4A-E). Nevertheless, *NUC1* loss-of-function suppressed *tps1Δ*-induced DNA fragmentation, while no statistical difference could be observed between *tps1Δ aif1Δ* and *tps1Δ* cells. The yeast caspase Yca1p also appeared as a mediator of some of the *tps1Δ*-related apoptotic traits, as the deletion of *YCA1* utterly eliminated caspase activity, suppressed membrane modifications, and reduced positive cells for ROS accumulation from 40 to 25% of cell population. However, *YCA1* deletion was without effect on the viability and percentage of cells with mitochondria hyperpolarization, providing another example of cell death triggering that depends only partially on caspase action (Madeo et al., 2009).

All single and double disruptants grown to exponential phase were then exposed to AA 120 mM and H_2O_2 10 mM, respectively (Fig. 5). As in Figure 3, we considered in calculations the initial apoptotic states of the different mutants in the exponential phase, to visualize the sole effect of stress exposure. When analyzing consequences of gene deletions in the *tps1Δ* background that strongly sensitized cells to stress, *yca1Δ* was the only mutation able to suppress AA-triggered apoptosis. This double *yca1Δ tps1Δ* disruptant exhibited features of

the single *yca1Δ* mutant and unambiguously supported a caspase-dependent pathway for AA-induced cell death. With regard to the peroxide exposure assay, both *NUC1* and *AIF1* deletions significantly limited the sensitivity of *tps1Δ* cells. They led to a drop of viability and an increase in the number of cells with AnV/PI co-staining comparable to those observed in the WT strain. However, neither *nuc1Δ* nor *aif1Δ* in this *tps1Δ* background was able to prevent peroxide-induced DNA fragmentation, contrary to what was observed in the *TPS1* context, where these single disruptants blocked the rise in positive cells for DNA fragmentation. In contrast to *NUC1* and *AIF1* deletions, neither *YCA1* nor *NDI1* deletion helped *tps1Δ* strains to better survive this harmful, peroxide-triggered oxidative stress.

3.6. The occurrence of apoptosis in *tps1Δ* cells correlated with a rapid drop of ATP levels

It is well known that a *tps1*Δ mutant cannot maintain its ATP levels, notably in response to glucose exposure (Walther et al., 2013) and when under heat stress (Petitjean et al., 2015). Likewise, we observed that exposure of *tps1*Δ cells to the lower doses of AA and peroxide caused an irreversible drop of ATP levels, in less than 3 hours (Fig. 6A and 6B). A continuous drop of the ATP charge was also noticed during growth of the *tps1*Δ mutant strain (Fig. 6C), (see the decrease of ATP levels from A_{600} 1.0 (early exponential) to A_{600} 3.0 (late exponential)), with full depletion of this crucial metabolite even before the onset of the diauxic shift. Conversely, this ATP charge remained high in the WT and *tps1-156* strains.

4. DISCUSSION

Trehalose does not prevent the loss of viability and commitment to apoptosis.

The disaccharide trehalose has been reported as an essential component in yeast longevity (Kyryakov et al., 2012; Samokhvalov et al., 2004a) and in the inhibition of apoptosis (Hu et al., 2014; Kyryakov et al., 2012; Lu et al., 2011). By way of example, it has been suggested as a negative regulator of peroxide-induced apoptosis, through the inhibition of Ca2+ signaling pathway and caspase activity (Lu et al., 2011). We revisited these conclusions in the present work, as we recently showed that the trehalose-6-phosphate synthase (Tps1 protein) was the main determinant for stress resistance in yeast (Gibney et al., 2015; Petitjean et al., 2015), contrary to long-standing claims on the essential role of trehalose in stress resistance (Elbein et al., 2003). By using the same experimental strategy (Petitjean et al., 2015), especially the expression of a catalytically inactive variant of Tps1p, we proved that it is the lack of Tps1 protein, and not that of trehalose, which significantly reduces chronological lifespan and hypersensitizes yeast cells to external apoptotic stimuli (*e.g.* acetic acid and peroxide). Interestingly, we also found that the Tps1 protein, and not trehalose, was able to prevent spontaneous apoptotic cell death during exponential growth. This useless role of trehalose was consistent with the absence of intracellular trehalose during the exponential growth of WT cells (Parrou et al., 1999). These results highlighted the potential pitfalls of both correlation-based studies and the use of gene deletions (*e.g. tps1*Δ), strengthening the idea that correlation is not causality. In light of these and previous results (Wilson et al., 2007; Petitjean et al., 2015), affirmations of trehalose function that have been raised based on *TPS1* deletion in any fungal species, must be carefully revisited.

The lack of the Tps1 protein leads to stochastic commitment to cell death and variable population growth rate.

Our preliminary observations suggest that living *tps1*Δ cells divide almost as fast as the WT cells, the low growth rate of the population being explained by the significant fraction of cells that commit to cell death. Interestingly, the high culture-to-culture growth rate variation that we noticed for *tps1*Δ cells, was also observed in perfectly controlled bioreactors (our unpublished data), which minimizes the possible influence of extrinsic factors. It fits instead with published reports that heterogeneity in growth rate, even for genetically identical cells, can be propagated over several generations (Kelly and Rahn, 1932; Wheals and Lord, 1992). A very recent work by Cerulus et al. (2016) quantified this phenomenon and demonstrated that clonal populations that are growing in the exponential phase could show considerable heterogeneity and epigenetic inheritance of single-cell doubling times, possibly leading to heterogeneity of population growth rate. Whether, in the absence of the Tps1 protein, both stochastic commitment to cell death and heterogeneous doubling times between the remaining living-cells explain such culture-to-culture growth rate variation, should deserve further investigations.

The lack of Tps1p affects apoptosis through cell death executioners' dependent and independent pathways.

Negative regulators of apoptosis have been described in yeast (Owsianowski et al., 2008). Only in a few cases, *e.g. CDC48*, *ASF1*, *LSM4* or *UBP10* (Bettiga et al., 2004; Madeo et al., 1997; Mazzoni et al., 2003; Yamaki et al., 2001), loss-of-function of the gene committed cells to apoptosis during exponential growth. The pro-survival role of Tps1p, remarkably illustrated by the spontaneous commitment to apoptosis of exponentially growing *tps1*Δ cells, indicated that the very small amount of Tps1p present during growth (Ghaemmaghami et al., 2003; Parrou et al., 1999) is sufficient to guarantee this function in WT cells. Further, this small intracellular level of Tps1 was not only sufficient, but also optimal if remembering that the

overexpression of *TPS1*, through T6P overaccumulation, appeared somewhat antagonistic to the positive effect of the Tps1 protein itself. However, by increasing the amount of the $Tps1^{D156G}$ variant, AA-triggered apoptosis was very nearly abolished. Our data thus evidenced that in a WT strain, Tps1p could interfere with AA-triggered cell death signaling. The TOR pathway is an appealing target, as it was recently reported as an important regulatory node during AA-induced apoptosis (Almeida et al., 2009).

Among downstream players of the apoptotic pathways that were analyzed for their putative involvement in *tps1Δ*-triggered cell death, the deletion *of AIF1, NUC1* and *YCA1* partially rescued *tps1Δ* phenotypes during the exponential growth. The deletion of *YCA1* suppressed caspase activity and membrane modifications. However, the fact that viability and other apoptotic markers remained altered as in the single *tps1Δ* strain during growth, provided another example of cell death process that depends only partially on caspase action (Madeo et al., 2009). The deletion of *YCA1* was however able to fully suppress AA-triggered apoptosis, even in the highly sensitive *tps1Δ* background, which unambiguously supported a caspase-dependent pathway for AA-induced cell death.

The comparable effects of *AIF1* and *NUC1* deletions supported the idea that *tps1Δ*-triggered cell death execution during the exponential growth relies, at least to some extent, upon these key effectors. But the translocation of Aif1p from mitochondria to the nucleus was questionable, as we did not observe any effect on chromatin fragmentation levels while deleting *AIF1,* contrary to what was observed for *NUC1* deletion. Under peroxide-triggered apoptosis, the viability of *tps1Δ* was only restored by the deletion of *AIF1* or *NUC1*. However, these deletions did not block the significant rise in the number of cells exhibiting DNA fragmentation, reinforcing the idea that Aif1p and Nuc1p mutually compensate for

vitality under various conditions of environmental stress and endogenous-induced apoptosis (Büttner et al., 2007b).

Finally, we analyzed the putative role of Ndi1p in *tps1Δ*-triggered ROS accumulation, as dysfunctional mitochondria are most routinely cited as the major source of mitochondrial ROS (Cui et al., 2012; Li, 2006). Against all odds, this protein did not appear to mediate *tps1Δ*-triggered cell death, as the *tps1Δ ndi1Δ* double mutant perfectly clustered with the *tps1Δ* strain, maintaining high levels of ROS positive cells. This result raised the possibility that ROS production may arise from the ER-localized NADPH oxidase, Yno1p (Rinnerthaler et al., 2012), which accounted for the majority of detectable ROS in the context of reduced cytochrome c oxidase (COX) activity (Leadsham et al., 2013).

The clear-cut apoptotic phenotypes of the *tps1Δ* strain are independent of the permissive carbon source.

The most outstanding phenotype of the *tps1*Δ mutant is its inability to grow on rapidly assimilated carbon sources (*e.g.* glucose or fructose), galactose being therefore the usual, permissive carbon source used to cultivate this mutant strain. Clear-cut apoptotic phenotypes of the *tps1*Δ strain were observed during early exponential growth, independently of the nature of the permissive carbon source used (*i.e.* respiratory, or respiro-fermentative as galactose (our unpublished data and (Fendt and Sauer, 2010; Ostergaard et al., 2000a, 2000b, 2001; Syriopoulos et al., 2008)). This result contrasted with the *nuc1*Δ strain whose phenotypes were qualified as subtle; either protecting against, or sensitizing to, stress-triggered cell death when the strain was grown in glycerol or glucose respectively (Büttner et al., 2007b). In our study however, even if they grew on galactose and fermented, we did not observe any apoptotic markers for *nuc1*Δ cells that clustered with the WT strain, contrary to what might have been expected from these cells grown on glucose (Büttner et al., 2007b). A few, similar discrepancies could be noticed for some of the single mutants exposed to

apoptotic stimuli (Fig. 5). We still don't know whether the carbon source is the only reason for those variations, as different genetic backgrounds or any other, undetermined factor may also affect the occurrence of few of these specific apoptotic features. For that reason, we at least duplicated, and validated, all results in the BY background, for the WT, *tps1Δ* and *tps1-156* strains, under all relevant conditions of the study.

The pro-survival role of the Tps1 protein probably relies on the maintenance of ATP homeostasis, but not only

In previous works, we reported that a *tps1*Δ strain cannot maintain ATP levels under environmental changes (Petitjean et al., 2015; Walther et al., 2013). Interestingly, declining ATP levels and redox alteration were considered as potential causes of regulated cell death (Galluzzi et al., 2015; Pereira et al., 2010; Sousa et al., 2013). We can, therefore, argue that part of the pro-survival function of the Tps1 protein may rely on the capacity to preserve ATP levels under apoptotic stimuli; hence providing substrate to 'ATP hungry' proteins. By way of example, we may cite proteins as Cdc48p, which belong to the class of AAA+ proteins (ATPases associated with various cellular activities) and are components of the machinery necessary for maintaining cell integrity. Also, failure to stabilize ATP levels in the *tps1*Δ background may affect ATP-dependent processes, as actin cytoskeleton dynamics, whose regulation has been shown to influence the decision to commit to apoptosis (Gourlay and Ayscough, 2005a, 2005b; Gourlay et al., 2004, 2006; Leadsham et al., 2010; Smethurst et al., 2014).

However, perturbation of the energy status of the cell may not be considered as the sole reason for apoptotic cell death of the *tps1*Δ strain, as early exponentially growing cells committed to apoptosis, while they showed almost wild type ATP levels. These data, together with the possible interaction of Tps1p with the TOR pathway during AA-induced apoptosis (see above), indicate that the function of Tps1p implicates specific targets that remain to be

identified. We recently demonstrated that the Tps1 protein itself is crucial for cell integrity under stress exposure as heat shock (Petitjean et al., 2015), independently of apoptotic cell death processes (data not shown). These new results provide unbiased evidence for an alternative function of this protein as anti-apoptotic factor, and allowed us to further confirm the idea that Tps1p is a moonlighting protein (Flores and Gancedo, 2011; Gancedo and Flores, 2008).

Conclusions

The search for pro-survival factors is relevant for improving stress resistance and preventing cell death of microbial cells under industrial processes. Here, the Tps1 protein and its interplay with apoptotic processes delineates novel targets for the selection and engineering of more robust industrial strains. Conversely, Almeida et al. (2008) reported the urgent need for a new generation of antifungal drugs that could enable the specific manipulation of yeast cell death, without causing side effects on human cells. Despite the high conservation of cell death processes between yeasts and mammals, our finding that yeast apoptotic cell death was greatly accelerated upon deletion of *TPS1* could fulfil this need, since the Tps1 protein is only present in bacteria, fungi and plants, but absent in mammals. Together with the key function of the Tps1 protein in providing tolerance to hostile environments (Petitjean et al., 2015), this architectural difference between apoptotic regulators of yeast and mammalian cells appeared as a possible Achilles' heel of yeast. Beyond *S. cerevisiae*, the Tps1 protein could therefore represent an appealing target for the selective destruction of closely related pathogens (*e.g. Candida albicans*) and evolutionarily more distant fungi (*e.g. A. fumigatus*).

Acknowledgements

We are grateful to Paula Ludovico (Life and Health Sciences Research Institute (ICVS), Braga, Portugal) for generously providing the pYX222-mtDsRed plasmid, and to Gustavo De Billerbeck (LISBP, Université de Toulouse, Toulouse, France) for the analysis of yeast growth kinetics. Marjorie Petitjean was supported by a doctoral grant from the French Ministry of Education and Research. The authors of this manuscript have no conflict of interests to declare.

Supplementary data

Figures S1 - S3 and Tables S1 - S5

References

Aerts, A.M., Zabrocki, P., François, I.E.J.A., Carmona-Gutierrez, D., Govaert, G., Mao, C., Smets, B., Madeo, F., Winderickx, J., Cammue, B.P.A., Thevissen, K., 2008. Ydc1p ceramidase triggers organelle fragmentation, apoptosis and accelerated ageing in yeast. Cell. Mol. Life Sci. 65, 1933–1942.

Allen, C., Büttner, S., Aragon, A.D., Thomas, J.A., Meirelles, O., Jaetao, J.E., Benn, D., Ruby, S.W., Veenhuis, M., Madeo, F., Werner-Washburne, M., 2006. Isolation of quiescent and nonquiescent cells from yeast stationary-phase cultures. The Journal of Cell Biology 174, 89–100.

Almeida, B., Ohlmeier, S., Almeida, A.J., Madeo, F., Leão, C., Rodrigues, F., Ludovico, P., 2009. Yeast protein expression profile during acetic acid-induced apoptosis indicates causal involvement of the TOR pathway. Proteomics 9, 720–732.

Almeida, B., Silva, A., Mesquita, A., 2008. Drug-induced apoptosis in yeast. Biochimica et Biophysica Acta (BBA) 1783, 1436-48.

Amigoni, L., Martegani, E., Colombo, S., 2013. Lack of *HXK2* induces localization of active Ras in mitochondria and triggers apoptosis in the yeast *Saccharomyces cerevisiae*. Oxid Med Cell Longev 2013, 678473.

Ayer, A., Gourlay, C.W., Dawes, I.W., 2014. Cellular redox homeostasis, reactive oxygen species and replicative ageing in *Saccharomyces cerevisiae*. FEMS Yeast Res 14, 60–72.

Bettiga, M., Calzari, L., Orlandi, I., Alberghina, L., Vai, M., 2004. Involvement of the yeast metacaspase Yca1 in ubp10Delta-programmed cell death. FEMS Yeast Res 5, 141–147.

Blazquez, M.A., Lagunas, R., Gancedo, C., Gancedo, J.M., 1993. Trehalose-6-phosphate, a new regulator of yeast glycolysis that inhibits hexokinases. FEBS Lett. 329, 51–54.

Braun, R.J., Westermann, B., 2011. Mitochondrial dynamics in yeast cell death and aging. Biochemical Society transactions 39, 1520–1526.

Breitenbach, M., Rinnerthaler, M., Hartl, J., Stincone, A., Vowinckel, J., Breitenbach-Koller, H., Ralser, M., 2014. Mitochondria in ageing: there is metabolism beyond the ROS. FEMS Yeast Res 14, 198–212.

Büttner, S., Carmona-Gutierrez, D., Vitale, I., Castedo, M., Ruli, D., Eisenberg, T., Kroemer, G., Madeo, F., 2007a. Depletion of endonuclease G selectively kills polyploid cells. Cell Cycle 6, 1072–1076.

Büttner, S., Eisenberg, T., Carmona-Gutierrez, D., Ruli, D., Knauer, H., Ruckenstuhl, C., Sigrist, C., Wissing, S., Kollroser, M., Fröhlich, K.-U., Sigrist, S., Madeo, F., 2007b. Endonuclease G regulates budding yeast life and death. Mol. Cell 25, 233–246.

Büttner, S., Eisenberg, T., Herker, E., Carmona-Gutierrez, D., Kroemer, G., Madeo, F., 2006. Why yeast cells can undergo apoptosis: death in times of peace, love, and war. The Journal of Cell Biology 175, 521–525.

Carmona-Gutierrez, D., Eisenberg, T., Büttner, S., Meisinger, C., Kroemer, G., Madeo, F., 2010. Apoptosis in yeast: triggers, pathways, subroutines. Cell Death Differ. 17, 763–773.

Cerulus, B., New, A.M., Pougach, K., Verstrepen, K.J., 2016. Noise and Epigenetic Inheritance of Single-Cell Division Times Influence Population Fitness. Current biology 26, 1138–1147.

Cui, Y., Zhao, S., Wu, Z., Dai, P., Zhou, B., 2012. Mitochondrial release of the NADH dehydrogenase Ndi1 induces apoptosis in yeast. Mol. Biol. Cell 23, 4373–4382.

Silva, A., Almeida, B., Sampaio-Marques, B., Reis, M.I., Ohlmeier, S., Rodrigues, F., Vale, A., Ludovico, P., 2011. Glyceraldehyde-3-phosphate dehydrogenase (GAPDH) is a specific substrate of yeast metacaspase. Biochim Biophys Acta. 1813, 2044-2049.

Eisenberg, T., Schroeder, S., Andryushkova, A., Pendl, T., Küttner, V., Bhukel, A., Mariño, G., Pietrocola, F., Harger, A., Zimmermann, A., Moustafa, T., Sprenger, A., Jany, E., Büttner, S., Carmona-Gutierrez, D., Ruckenstuhl, C., Ring, J., Reichelt, W., Schimmel, K., Leeb, T., Moser, C., Schatz, S., Kamolz, L.-P., Magnes, C., Sinner, F., Sedej, S., Fröhlich, K.-U., Juhasz, G., Pieber, T.R., Dengjel, J., Sigrist, S.J., Kroemer, G., Madeo, F., 2014. Nucleocytosolic depletion of the energy metabolite acetyl-coenzyme A stimulates autophagy and prolongs lifespan. Cell Metab. 19, 431–444.

Elbein, A.D., Pan, Y.T., Pastuszak, I., Carroll, D., 2003. New insights on trehalose: a multifunctional molecule. Glycobiology 13, 17R–27R.

Fabrizio, P., Battistella, L., Vardavas, R., Gattazzo, C., Liou, L.-L., Diaspro, A., Dossen, J.W., Gralla,

E.B., Longo, V.D., 2004. Superoxide is a mediator of an altruistic aging program in *Saccharomyces cerevisiae*. J. Cell Biol. 166, 1055–1067.
Fabrizio, P., Longo, V.D., 2003. The chronological life span of *Saccharomyces cerevisiae*. Aging cell 2, 73–81.
Favre, C., Aguilar, P.S., Carrillo, M.C., 2008. Oxidative stress and chronological aging in glycogen-phosphorylase-deleted yeast. Free Radic. Biol. Med. 45, 1446–1456.
Fendt, S.-M., Sauer, U., 2010. Transcriptional regulation of respiration in yeast metabolizing differently repressive carbon substrates. BMC Syst Biol 4, 12.
Flores, C.-L., Gancedo, C., 2011. Unraveling moonlighting functions with yeasts. IUBMB Life 63, 457–462.
François, J., Parrou, J.L., 2001. Reserve carbohydrates metabolism in the yeast *Saccharomyces cerevisiae*. FEMS Microbiology Reviews 25, 125–145.
Galluzzi, L., Bravo-San Pedro, J. M., Vitale, I., Aaronson, S.A., Abrams, J.M., et al., 2015. Essential versus accessory aspects of cell death: recommendations of the NCCD 2015. Cell Death Differ. 22, 58–73.
Gancedo, C., Flores, C.-L., 2004. The importance of a functional trehalose biosynthetic pathway for the life of yeasts and fungi. FEMS Yeast Res. 4, 351–359.
Gancedo, C., Flores, C.-L., 2008. Moonlighting proteins in yeasts. Microbiol. Mol. Biol. Rev. 72, 197–210.
Ghaemmaghami, S., Huh, W.-K., Bower, K., Howson, R.W., Belle, A., Dephoure, N., O'Shea, E.K., Weissman, J.S., 2003. Global analysis of protein expression in yeast. Nature 425, 737–741.
Giannattasio, S., Guaragnella, N., Corte-Real, M., 2005. Acid stress adaptation protects *Saccharomyces cerevisiae* from acetic acid-induced programmed cell death. Gene 354, 93-98.
Gibney, P.A., Schieler, A., Chen, J.C., Rabinowitz, J.D., Botstein, D., 2015. Characterizing the in vivo role of trehalose in *Saccharomyces cerevisiae* using the *AGT1* transporter. Proc. Natl. Acad. Sci. U.S.A. 112, 6116–6121.
González, M.I., Stucka, R., Blazquez, M.A., Feldmann, H., Gancedo, C., 1992. Molecular cloning of *CIF1*, a yeast gene necessary for growth on glucose. Yeast 8, 183–192.
Gourlay, C.W., Ayscough, K.R., 2005a. A role for actin in aging and apoptosis. Biochemical Society transactions 33, 1260–1264.
Gourlay, C.W., Ayscough, K.R., 2005b. The actin cytoskeleton: a key regulator of apoptosis and ageing? Nature reviews. Molecular cell biology 6, 583–589.
Gourlay, C.W., Carpp, L.N., Timpson, P., Winder, S.J., Ayscough, K.R., 2004. A role for the actin cytoskeleton in cell death and aging in yeast. The Journal of Cell Biology 164, 803–809.
Gourlay, C.W., Du, W., Ayscough, K.R., 2006. Apoptosis in yeast–mechanisms and benefits to a unicellular organism. Mol. Microbiol. 62, 1515–1521.
Greenwood, M.T., Ludovico, P., 2010. Expressing and functional analysis of mammalian apoptotic regulators in yeast. Cell Death Differ. 17, 737–745.
Guaragnella, N., Zdralević, M., Antonacci, L., Passarella, S., Marra, E., Giannattasio, S., 2012. The role of mitochondria in yeast programmed cell death. Front. Oncology 2, 70.
Guillou, V., Plourde-Owobi, L., Parrou, J.-L., Goma, G., François, J., 2004. Role of reserve carbohydrates in the growth dynamics of *Saccharomyces cerevisiae*. FEMS Yeast Res. 4, 773–787.
Herker, E., Jungwirth, H., Lehmann, K.A., Maldener, C., Fröhlich, K.-U., Wissing, S., Büttner, S., Fehr, M., Sigrist, S., Madeo, F., 2004. Chronological aging leads to apoptosis in yeast. The Journal of Cell Biology 164, 501–507.
Hohmann, S., Bell, W., Neves, M.J., Valckx, D., Thevelein, J.M., 1996. Evidence for trehalose-6-phosphate-dependent and -independent mechanisms in the control of sugar influx into yeast glycolysis. Mol. Microbiol. 20, 981–991.
Hu, J., Wei, M., Mirzaei, H., Madia, F., Mirisola, M., Amparo, C., Chagoury, S., Kennedy, B., Longo, V.D., 2014. Tor-Sch9 deficiency activates catabolism of the ketone body-like acetic acid to promote trehalose accumulation and longevity. Aging cell 13, 457–467.
Hughes, A.L., Gottschling, D.E., 2012. An early age increase in vacuolar pH limits mitochondrial function and lifespan in yeast. Nature 492, 261–265.
Jones, G.M., Stalker, J., Humphray, S., West, A., Cox, T., Rogers, J., Dunham, I., Prelich, G., 2008. A

systematic library for comprehensive overexpression screens in *Saccharomyces cerevisiae*. Nat. Methods 5, 239–241.
Jules, M., François, J., Parrou, J.-L., 2005. Autonomous oscillations in *Saccharomyces cerevisiae* during batch cultures on trehalose. The FEBS journal 272, 1490–1500.
Jules, M., Guillou, V., François, J., Parrou, J.-L., 2004. Two distinct pathways for trehalose assimilation in the yeast *Saccharomyces cerevisiae*. Appl. Environ. Microbiol. 70, 2771–2778.
Kelly, C.D., Rahn, O., 1932. The Growth Rate of Individual Bacterial Cells. J Bacteriol. 23, 147–153.
Kyryakov, P., Beach, A., Richard, V.R., Burstein, M.T., Leonov, A., Levy, S., Titorenko, V.I., 2012. Caloric restriction extends yeast chronological lifespan by altering a pattern of age-related changes in trehalose concentration. Front. Physiol. 3, 256.
Leadsham, J.E., Kotiadis, V.N., Tarrant, D.J., 2010. Apoptosis and the yeast actin cytoskeleton. Cell Death & Differentiation 17, 754-62.
Leadsham, J.E., Sanders, G., Giannaki, S., Bastow, E.L., Hutton, R., Naeimi, W.R., Breitenbach, M., Gourlay, C.W., 2013. Loss of cytochrome c oxidase promotes RAS-dependent ROS production from the ER resident NADPH oxidase, Yno1p, in yeast. Cell Metab. 18, 279–286.
Li, W., 2006. Yeast AMID Homologue Ndi1p Displays Respiration-restricted Apoptotic Activity and Is Involved in Chronological Aging. Mol. Biol. Cell 17, 1802–1811.
Liang, Q., Li, W., Zhou, B., 2008. Caspase-independent apoptosis in yeast. Biochimica et Biophysica Acta (BBA) 1783, 1311-9.
Longo, V.D., Fabrizio, P., 2002. Regulation of longevity and stress resistance: a molecular strategy conserved from yeast to humans? Cell. Mol. Life Sci. 59, 903–908.
Longo, V.D., Fabrizio, P., 2012. Chronological aging in *Saccharomyces cerevisiae*. Subcell. Biochem. 57, 101–121.
Lu, H., Zhu, Z., Dong, L., Jia, X., Sun, X., Yan, L., Chai, Y., Jiang, Y., Cao, Y., 2011. Lack of trehalose accelerates H2O2-induced *Candida albicans* apoptosis through regulating Ca2+ signaling pathway and caspase activity. PLoS ONE 6, e15808.
Ludovico, P., Madeo, F., Silva, M., 2005. Yeast programmed cell death: an intricate puzzle. IUBMB Life 57, 129–135.
Ludovico, P., Rodrigues, F., Almeida, A., Silva, M.T., Barrientos, A., Côrte-Real, M., 2002. Cytochrome c release and mitochondria involvement in programmed cell death induced by acetic acid in *Saccharomyces cerevisiae*. Mol. Biol. Cell 13, 2598–2606.
Ludovico, P., Sansonetty, F., Corte-Real, M., 2001a. Assessment of mitochondrial membrane potential in yeast cell populations by flow cytometry. Microbiology 147, 3335–3343.
Ludovico, P., Sousa, M.J., Silva, M.T., Leão, C., Corte-Real, M., 2001b. *Saccharomyces cerevisiae* commits to a programmed cell death process in response to acetic acid. Microbiology 147, 2409–2415.
Madeo, F., 1999. Oxygen Stress: A Regulator of Apoptosis in Yeast. The Journal of Cell Biology 145, 757–767.
Madeo, F., Carmona-Gutierrez, D., Ring, J., Büttner, S., Eisenberg, T., Kroemer, G., 2009. Caspase-dependent and caspase-independent cell death pathways in yeast. Biochem. Biophys. Res. Commun. 382, 227–231.
Madeo, F., Fröhlich, E., Fröhlich, K.U., 1997. A yeast mutant showing diagnostic markers of early and late apoptosis. The Journal of Cell Biology 139, 729–734.
Madeo, F., Herker, E., Maldener, C., Wissing, S., Lächelt, S., 2002. A caspase-related protease regulates apoptosis in yeast. Mol. Cell. 9, 911–917.
Madeo, F., Herker, E., Wissing, S., Jungwirth, H., 2004. Apoptosis in yeast. Current opinion in microbiology. 7, 655-60.
Mazzoni, C., Falcone, C., 2008. Caspase-dependent apoptosis in yeast. Biochimica et Biophysica Acta (BBA). 1783, 1320-7.
Mazzoni, C., Mancini, P., Verdone, L., Madeo, F., Serafini, A., Herker, E., Falcone, C., 2003. A truncated form of KlLsm4p and the absence of factors involved in mRNA decapping trigger apoptosis in yeast. Mol. Biol. Cell 14, 721–729.
Mazzoni, C., Torella, M., Petrera, A., Palermo, V., Falcone, C., 2009. *PGK1*, the gene encoding the glycolitic enzyme phosphoglycerate kinase, acts as a multicopy suppressor of apoptotic phenotypes in *S. cerevisiae*. Yeast 26, 31–37.

Mirisola, M.G., Braun, R.J., Petranovic, D., 2014. Approaches to study yeast cell aging and death. FEMS Yeast Res. 14, 109–118.
Mirzaei, H., Longo, V.D., 2014. Acetyl-CoA synthetase is a conserved regulator of autophagy and life span. Cell Metab. 19, 555–557.
Ocampo, A., Liu, J., Schroeder, E.A., Shadel, G.S., Barrientos, A., 2012. Mitochondrial respiratory thresholds regulate yeast chronological life span and its extension by caloric restriction. Cell Metab. 16, 55–67.
Orlandi, I., Casatta, N., Vai, M., 2012. Lack of Ach1 CoA-transferase triggers apoptosis and decreases chronological lifespan in yeast. Front. Oncology 2, 67.
Ostergaard, S., Olsson, L., Johnston, M., Nielsen, J., 2000a. Increasing galactose consumption by *Saccharomyces cerevisiae* through metabolic engineering of the *GAL* gene regulatory network. Nat. Biotechnol. 18, 1283–1286.
Ostergaard, S., Olsson, L., Nielsen, J., 2001. In vivo dynamics of galactose metabolism in *Saccharomyces cerevisiae*: metabolic fluxes and metabolite levels. Biotechnology and bioengineering 73, 412–425.
Ostergaard, S., Roca, C., Rønnow, B., Nielsen, J., Olsson, L., 2000b. Physiological studies in aerobic batch cultivations of *Saccharomyces cerevisiae* strains harboring the *MEL1* gene. Biotechnology and bioengineering 68, 252–259.
Owsianowski, E., Walter, D., Fahrenkrog, B., 2008. Negative regulation of apoptosis in yeast. Biochim Biophys Acta 1783, 1303–1310.
Palabiyik, B., Jafari Ghods, F., 2015. Role of Oxidative Stress Response and Trehalose Accumulation in the Longevity of Fission Yeast. Jundishapur J Microbiol 8, e16851.
Parrou, J.L., Enjalbert, B., Plourde, L., Bauche, A., Gonzalez, B., François, J., 1999. Dynamic responses of reserve carbohydrate metabolism under carbon and nitrogen limitations in *Saccharomyces cerevisiae*. Yeast 15, 191–203.
Parrou, J.L., François, J., 1997. A simplified procedure for a rapid and reliable assay of both glycogen and trehalose in whole yeast cells. Anal. Biochem. 248, 186–188.
Pereira, C., Chaves, S., Alves, S., Salin, B., Camougrand, N., Manon, S., Sousa, M.J., Côrte-Real, M., 2010. Mitochondrial degradation in acetic acid-induced yeast apoptosis: the role of Pep4 and the ADP/ATP carrier. Mol. Microbiol. 76, 1398–1410.
Petitjean, M., Teste, M.-A., François, J.M., Parrou, J.-L., 2015. Yeast trehalose-6P tolerance to various stresses relies on the synthase (Tps1) protein, not on trehalose. J. Biol. Chem. 290, 16177–16190.
Plourde-Owobi, L., Durner, S., Parrou, J.L., Wieczorke, R., Goma, G., François, J., 1999. *AGT1*, encoding an alpha-glucoside transporter involved in uptake and intracellular accumulation of trehalose in *Saccharomyces cerevisiae*. J Bacteriol 181, 3830–3832.
Rinnerthaler, M., Büttner, S., Laun, P., Heeren, G., Felder, T.K., Klinger, H., Weinberger, M., Stolze, K., Grousl, T., Hasek, J., Benada, O., Frydlova, I., Klocker, A., Simon-Nobbe, B., Jansko, B., Breitenbach-Koller, H., Eisenberg, T., Gourlay, C.W., Madeo, F., Burhans, W.C., Breitenbach, M., 2012. Yno1p/Aim14p, a NADPH-oxidase ortholog, controls extramitochondrial reactive oxygen species generation, apoptosis, and actin cable formation in yeast. Proc. Natl. Acad. Sci. U.S.A. 109, 8658–8663.
Ruckenstuhl, C., Carmona-Gutierrez, D., 2010. The sweet taste of death: glucose triggers apoptosis during yeast chronological aging. Aging 2, 643-649.
Samokhvalov, V., Ignatov, V., Kondrashova, M., 2004a. Reserve carbohydrates maintain the viability of *Saccharomyces cerevisiae* cells during chronological aging. Mech. Ageing Dev. 125, 229–235.
Samokhvalov, V.A., Mel'nikov, G.V., Ignatov, V.V., 2004b. The role of trehalose and glycogen in the survival of aging *Saccharomyces cerevisiae* cells. Microbiology (Mikrobiologiya) 73, 449–454.
Smethurst, D.G.J., Dawes, I.W., Gourlay, C.W., 2014. Actin - a biosensor that determines cell fate in yeasts. FEMS Yeast Res 14, 89–95.
Sousa, M., Duarte, A.M., Fernandes, T.R., Chaves, S.R., Pacheco, A., Leão, C., Côrte-Real, M., Sousa, M.J., 2013. Genome-wide identification of genes involved in the positive and negative regulation of acetic acid-induced programmed cell death in *Saccharomyces cerevisiae*. BMC Genomics 14, 838.
Swinnen, E., Ghillebert, R., Wilms, T., Winderickx, J., 2014. Molecular mechanisms linking the evolutionary conserved TORC1–Sch9 nutrient signaling branch to lifespan regulation in

Saccharomyces cerevisiae.. FEMS Yeast Res 14, 17–32.
Syriopoulos, C., Panayotarou, A., Lai, K., Klapa, M.I., 2008. Transcriptomic analysis of *Saccharomyces cerevisiae* physiology in the context of galactose assimilation perturbations. Mol Biosyst 4, 937–949.
Thevelein, J.M., Hohmann, S., 1995. Trehalose synthase: guard to the gate of glycolysis in yeast? Trends Biochem. Sci. 20, 3–10.
Trevisol, E.T.V., Panek, A.D., Mannarino, S.C., Eleutherio, E.C.A., 2011. The effect of trehalose on the fermentation performance of aged cells of *Saccharomyces cerevisiae*. Appl. Microbiol. Biotechnol. 90, 697–704.
Tsiatsiani, L., Van Breusegem, F., Gallois, P., Zavialov, A., Lam, E., Bozhkov, P.V., 2011. Metacaspases. Cell Death Differ. 18, 1279–1288.
Tulha, J., Faria-Oliveira, F., Lucas, C., Ferreira, C., 2012. Programmed cell death in S*accharomyces cerevisiae* is hampered by the deletion of *GUP1* gene. BMC Microbiol. 12, 80.
Uren, A.G., O'Rourke, K., Aravind, L.A., Pisabarro, M.T., Seshagiri, S., Koonin, E.V., Dixit, V.M., 2000. Identification of paracaspases and metacaspases: two ancient families of caspase-like proteins, one of which plays a key role in MALT lymphoma. Mol. Cell 6, 961–967.
Van Dijken, J.P., Bauer, J., Brambilla, L., Duboc, P., et al. 2000. An interlaboratory comparison of physiological and genetic properties of four *Saccharomyces cerevisiae* strains. Enzyme and Microbial technology. 26, 706-714.
van Heerden, J.H., Wortel, M.T., Bruggeman, F.J., Heijnen, J.J., Bollen, Y.J.M., Planqué, R., Hulshof, J., O'Toole, T.G., Wahl, S.A., Teusink, B., 2014. Lost in transition: start-up of glycolysis yields subpopulations of nongrowing cells. Science 343, 1245114.
Walther, T., Mtimet, N., Alkim, C., Vax, A., Loret, M.-O., Ullah, A., Gancedo, C., Smits, G.J., François, J.M., 2013. Metabolic phenotypes of *Saccharomyces cerevisiae* mutants with altered trehalose 6-phosphate dynamics. Biochem. J. 454, 227–237.
Walther, T., Novo, M., Rössger, K., Létisse, F., Loret, M.-O., Portais, J.-C., François, J.M., 2010. Control of ATP homeostasis during the respiro-fermentative transition in yeast. Mol Syst Biol 6, 344.
Wanichthanarak, K., Cvijovic, M., Molt, A., Petranovic, D., 2013. yApoptosis: yeast apoptosis database. Database (Oxford) 2013, bat068.
Wheals, A.E., Lord, P.G., 1992. Clonal heterogeneity in specific growth rate of *Saccharomyces cerevisiae* cells. Cell Prolif. 25, 217–223.
Wilson, R.A., Jenkinson, J.M., Gibson, R.P., Littlechild, J.A., Wang, Z.-Y., Talbot, N.J., 2007. Tps1 regulates the pentose phosphate pathway, nitrogen metabolism and fungal virulence. EMBO J. 26, 3673–3685.
Wissing, S., Ludovico, P., Herker, E., Büttner, S., Engelhardt, S.M., Decker, T., Link, A., Proksch, A., Rodrigues, F., Côrte-Real, M., Fröhlich, K.-U., Manns, J., Candé, C., Sigrist, S.J., Kroemer, G., Madeo, F., 2004. An AIF orthologue regulates apoptosis in yeast. The Journal of Cell Biology 166, 969–974.
Wloch-Salamon, D.M., Bem, A.E., 2013. Types of cell death and methods of their detection in yeast *Saccharomyces cerevisiae*. J. Appl. Microbiol. 114, 287–298.
Yamaki, M., Umehara, T., Chimura, T., Horikoshi, M., 2001. Cell death with predominant apoptotic features in *Saccharomyces cerevisiae* mediated by deletion of the histone chaperone *ASF1*/*CIA1*. Genes Cells 6, 1043–1054.

Figure legends

Figure 1: The deletion of *TPS1* triggers a massive apoptotic cell death during exponential growth

(A) Flow cytometry analysis of the percentage of viable cells and of positive cells for apoptotic markers during exponential growth. Strains were grown in YN Gal medium to A_{600} ~1.0. In addition to the three reference strains of this work (WT, *tps1Δ* and *tps1-156*), the *tps1Δ* strain was also transformed with a 2µ plasmid bearing the *tps1-156* and *TPS1* alleles, respectively (Strains #4 and #5). Stacked bars from the 'Membrane modifications' category gather together the percentages of positive cells for AnV staining (grey), AnV/PI co-staining (orange) and PI-only staining (green). The data are represented as means ± 2 SEM of three to five biological replicates. Results of the One-way ANOVA test for WT *vs*. *tps1Δ* (significance level of 1%) are given in Table S1.

(B) Analysis of mitochondrial morphology by confocal microscopy. To visualize mitochondrial network organization, *TPS1* and *tps1Δ* cells were transformed with the pYX222-mtDsRed plasmid. Single laser lines used for excitation were Diode Pumped Solid State Lasers (DPSSL) exciting DsRed at 561 nm (50 mW; Cobolt Jive). A bandpass emission filter (FF01-512/630-25, Semrock) allowed collection of the red fluorescence. Pixel size was 65 nm. 250-nm z step were used for the acquisition.

Figure 2: Chronological lifespan in strains affected for trehalose metabolism

(A) Survival of strains grown in YN Gal medium and left for 4 weeks at 30 °C, with continuous shaking. *Day* 0, start of the experiment (A_{600} ~1.0). Cells were also grown in the presence of trehalose (+, YN GalTre medium), but only the *tps1Δ* strain is shown for the sake of clarity. The data are represented as means ± 1 SEM of three independent replicates (*i.e.* different calendar periods).

(B–E) Percentage of positive cells for apoptotic markers after 9 and 22 days of chronological aging (*Day* 0 as reference). (B), Percent of positive cells for ROS accumulation; (C), Percent of cells presenting hyper- or depolarization of mitochondria (grey and orange, respectively); (D), Membrane modifications with percentage of positive cells for AnV staining (grey), AnV/PI co-staining (orange) and PI-only staining (green); (E), Percent of cells presenting caspase activity. The data are represented as means ± 2 SEM of three independent replicates. Results of the One-way ANOVA test for WT *vs. tps1Δ* (significance level of 1%) are given in Table S2.

Figure 3: Acetic acid and H_2O_2-triggered apoptosis in strains affected for trehalose metabolism

(A) "Drop of viability" after exposure to different concentrations of acetic acid (40 to 120 mM) and peroxide (1 to 10 mM). The "drop of viability" was calculated as the difference between the viability measured after exposure to the stress of interest for 4 hours, and the viability observed during exponential growth (A_{600} ~0.5-0.7). (B-E) "Changes in the number of positive cells" for apoptotic markers (%), calculated as the difference between values measured after exposure to the stress of interest for 4 hours, and the values measured during exponential growth. (B), ROS accumulation; (C), Hyper- or depolarization of mitochondria (grey and orange, respectively). Filled and dashed grey bars indicate respectively an increase and a decrease in the number of hyperpolarized cells; (D), Membrane modifications with AnV staining (grey), AnV/PI co-staining (orange) and PI-only staining (green); (E), Caspase activity (green) and DNA fragmentation (purple). The data are represented as means ± 2 SEM of three biological replicates. For the sake of clarity, statistics were not plotted but exhaustive results of the Two-way ANOVA test (significance level of 1%) could be found in Table S3.

Figure 4: Genetic interaction between *TPS1* and genes encoding executioners of apoptotic cell death in exponentially growing cells.

Hierarchical Ascendant Classification (HAC) of single and double mutants between *tps1Δ* and knockouts of known effectors of apoptosis. This Classification was performed according to the Ward method, with default parameters (standardization of the data and squared Euclidean distances), by using the whole set of quantitative data (*i.e.* viability and all apoptotic markers, presented in panels A–E and measured from cells grown to A_{600}~1.0 in YN Gal medium, with the exception of DNA fragmentation results that were not included in the analysis as solely evaluated for *nuc1Δ* and *aif1Δ* strains).

(A-E) Strains were ordered on the horizontal axis as obtained from the HAC. (A), Percent of viable cells; (B), Percent of positive cells for ROS accumulation; (C), Percent of cells with mitochondria hyper-polarization; (D), Membrane modifications with percent of positive cells for AnV staining (grey), AnV/PI co-staining (orange) and PI-only staining (green); (E), Positive cells presenting caspase activity (green) or showing DNA fragmentation (purple). The data are represented as means ± 2 SEM of three biological replicates. Results of the One-way ANOVA test for *tps1Δ vs.* double mutants (significance level of 1%) are given in Table S4.

Figure 5: Molecular machinery of *tps1Δ*-triggered cell death execution under acetic acid and peroxide exposure.

Legend as in Figure 3. (A), "drop of viability" after exposure to acetic acid 120 mM and peroxide 10 mM, for 4 hours. (B-E), Changes in the number of positive cells for apoptotic markers. (B), ROS accumulation; (C), hyper- or depolarization of mitochondria (grey and orange, respectively). Filled and dashed grey bars indicate respectively an increase and a decrease in the number of hyperpolarized cells; (D), Membrane modifications (AnV staining (grey), AnV/PI co-staining (orange) and PI-only staining (green)); (E), Caspase activity

(green) and DNA fragmentation (purple). The data are represented as means ± 2 SEM of three biological replicates (excepted for caspase and DNA fragmentation assays with only two biological replicates). For the sake of clarity, statistics were not plotted, but results of the Two-way ANOVA test for *tps1Δ vs.* double mutants (significance level of 1%) could be found in Table S5.

Figure 6: The Tps1 protein guarantees the maintain of ATP levels

Levels of ATP during exposure of yeast cells to acetic acid (A), peroxide (B), or during growth (C). (A) and (B), ATP as a function of exposure time; (C), ATP as a function of A_{600}. Data are represented as mean ± SD of 3 independent biological replicates.

Supplementary material for :

"**A new function for the yeast Trehalose-6P Synthase (Tps1) Protein, as key pro-survival factor during growth, chronological ageing, and apoptotic stress**."

Supplementary Figure Legends

Figure S1: Living *tps1* cells divide almost as fast as WT cells.

(A) Representative plot of the evolution of A_{600} as a function of time, during the exponential phase of growth. For each sample, we also measured the total cell number (N_t, *per* ml of culture), and the number of viable cells (N_v, *per* ml), which allowed us to calculate the viability as the ratio between viable cells (N_v) and the total number of cells (N_t). The exponential fitting curve enables to access the apparent specific growth rate of cell population (μ) during this exponential phase of growth. (B) Plot of the "*apparent*" specific growth rate (μ) as a function of the viability. Each point of the graph represents an independent culture, either from the WT (black) or of the *tps1*Δ strain (red). The viability value (x-axis) is the mean viability calculated from all samples analyzed during the exponential phase of growth. (C1-C4) indirect evaluation of the "*intrinsic*" growth rate (μ_i). (C1) At any time during growth, viable cells can either divide (intrinsic growth rate of dividing cells, μ_i), or die (death rate, μ_d). In a closed system (batch culture), and if considering a quasi-stationary state during this exponential phase (*i.e.* constant evolution rates μ_i & μ_d), the two differential equations (1) and (2) give the evolution of the viable cells, and of the total number of cells, respectively. The independent, integral forms of these equations (B2), enable to determine the two unknowns μ_i and μ_d; (C4), same as in (B), with the "*intrinsic*" specific growth rate (μ_i) as a function of viability.

Figure S2: Monitoring of Rh123-based mitochondrial membrane potential by flow cytometry.

Representative BL-1-RL-2 scatter plots of Rh123-stained cells (log scale, BL-1 (525 nm filter), RL-2 (665 nm filter)). (A) Plots obtained from exponentially growing cells (A_{600}~1) of the WT and *tps1*Δ strains. (B) Control assays for depolarization or hyperpolarization of mitochondria, after exposure of WT cells to FCCP 5 µM and Nigericin 5µM, respectively. Rh123-staining analysis was performed on BL-1, concluding for hyperpolarization when the cells presented a fluorescence signal above the 10^4-treshold, while cells with depolarized mitochondria led to a signal bellow 10^2 AU (AU, Arbitrary Units of fluorescence).

Figure S3: Comparative analysis of AA- and H_2O_2-triggered loss of viability, in CEN.PK and BY strain backgrounds.

"Drop of viability" after exposure to different concentrations of acetic acid (40 to 120 mM) and peroxide (1 to 10 mM). CEN.PK (upper graph) or BY strain background (lower graph). Legend as in Figure 3.

Figure

Figure 1

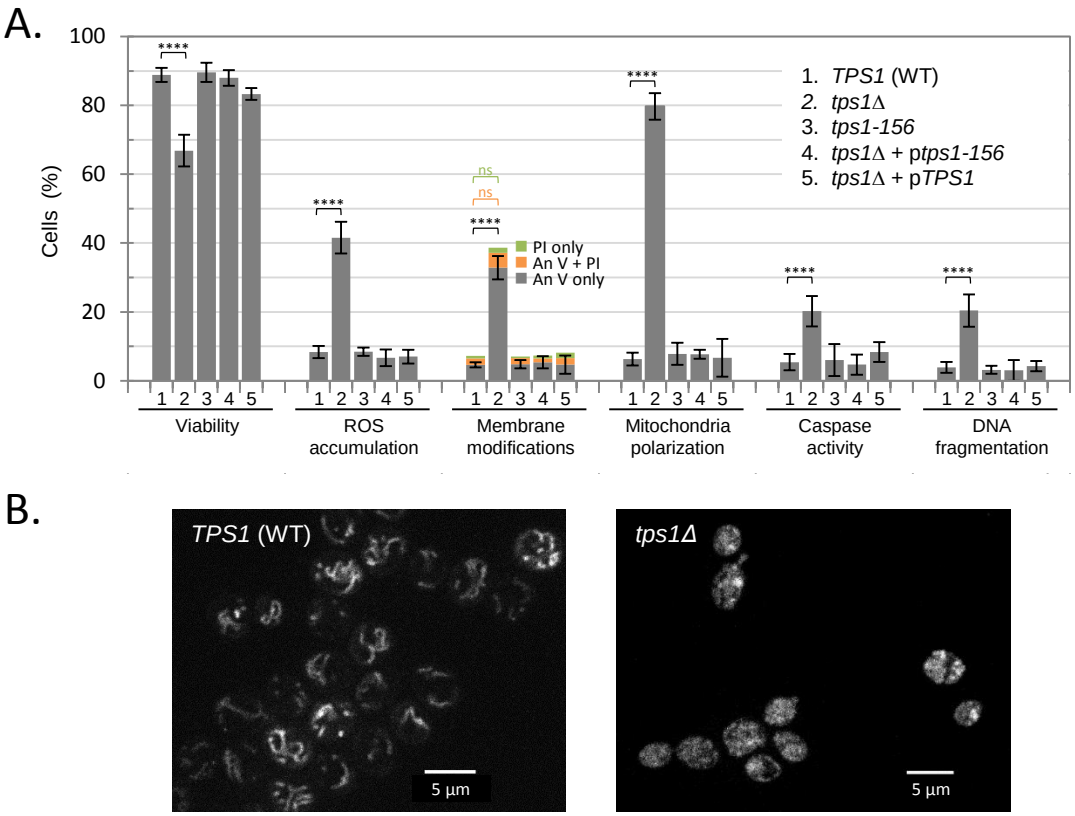

Figure 2

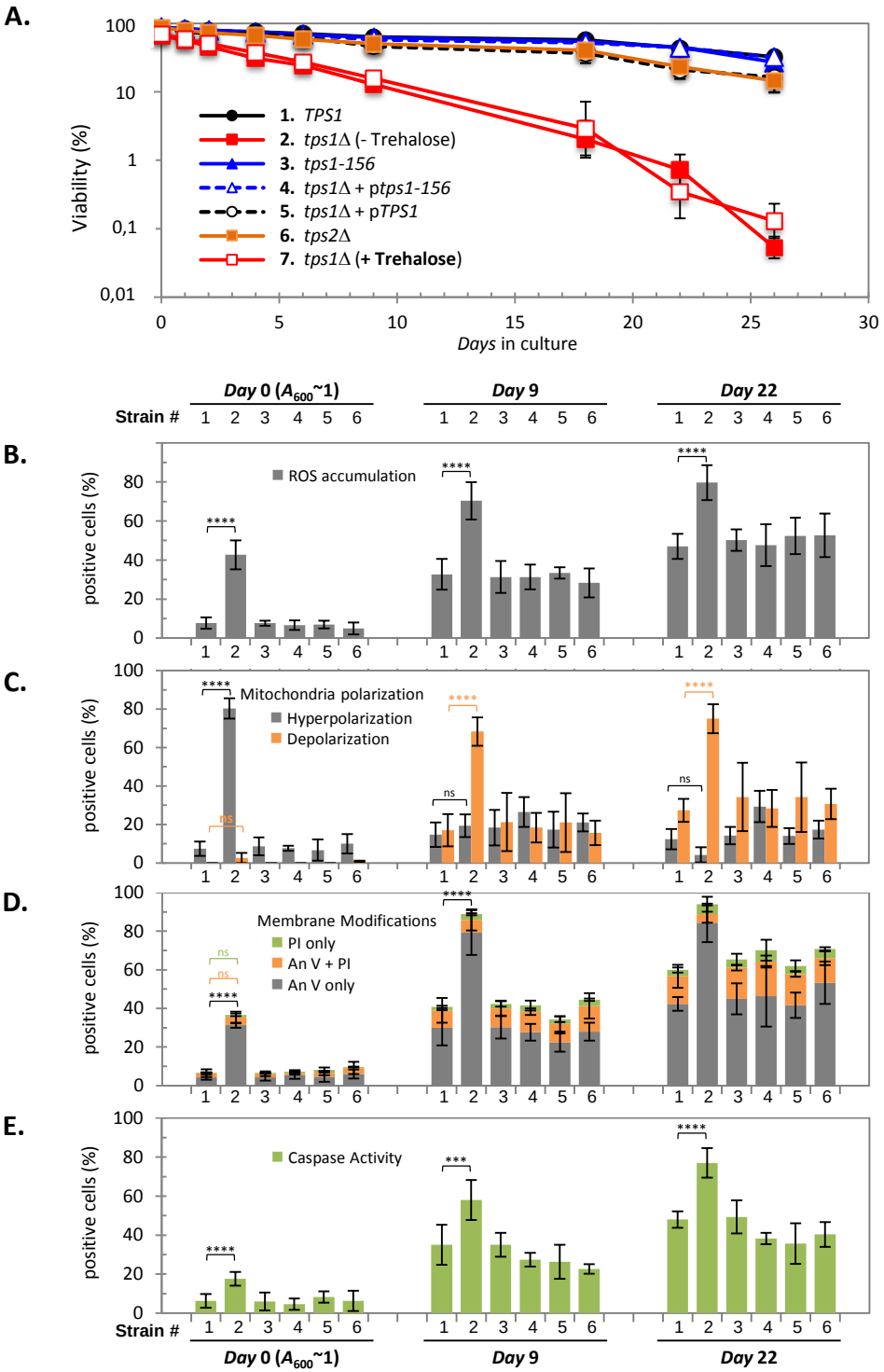
A.
Viability (%)
100
10
1
0,1
0,01
0
5
10
15
20
25
30
Days in culture
1. TPS1
2. tps1Δ (- Trehalose)
3. tps1-156
4. tps1Δ + ptps1-156
5. tps1Δ + pTPS1
6. tps2Δ
7. tps1Δ (+ Trehalose)
Day 0 (A600~1)
Day 9
Day 22
Strain # 1 2 3 4 5 6
B.
ROS accumulation
positive cells (%)
C.
Mitochondria polarization
Hyperpolarization
Depolarization
D.
Membrane Modifications
PI only
An V + PI
An V only
E.
Caspase Activity
****
***
ns

Figure 3

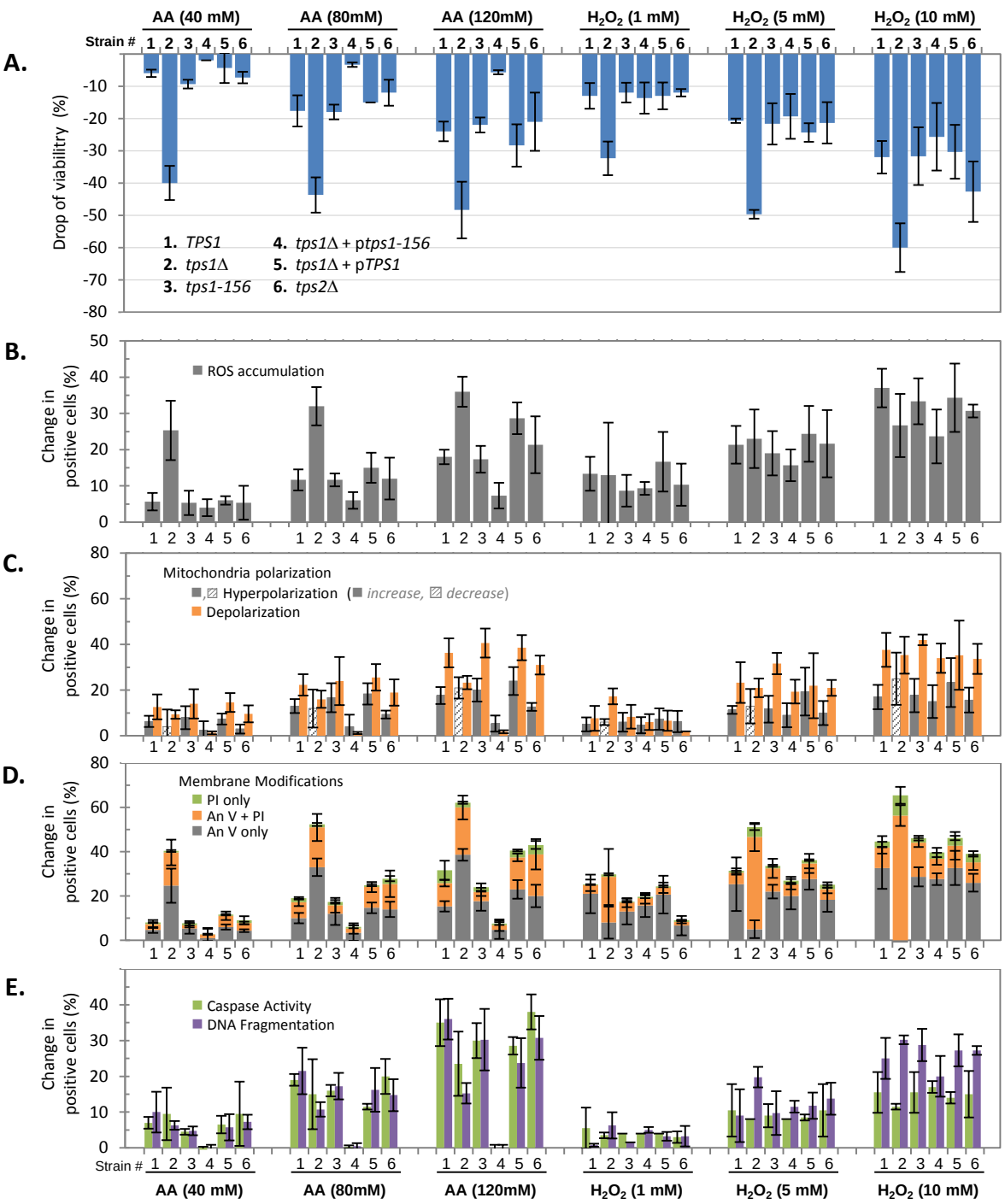
A.
AA (40 mM)
AA (80mM)
AA (120mM)
H2O2 (1 mM)
H2O2 (5 mM)
H2O2 (10 mM)
Strain # 1 2 3 4 5 6
Drop of viability (%)
1. TPS1
2. tps1Δ
3. tps1-156
4. tps1Δ + ptps1-156
5. tps1Δ + pTPS1
6. tps2Δ
B.
ROS accumulation
Change in positive cells (%)
C.
Mitochondria polarization
Hyperpolarization (increase, decrease)
Depolarization
D.
Membrane Modifications
PI only
An V + PI
An V only
E.
Caspase Activity
DNA Fragmentation

Figure 4

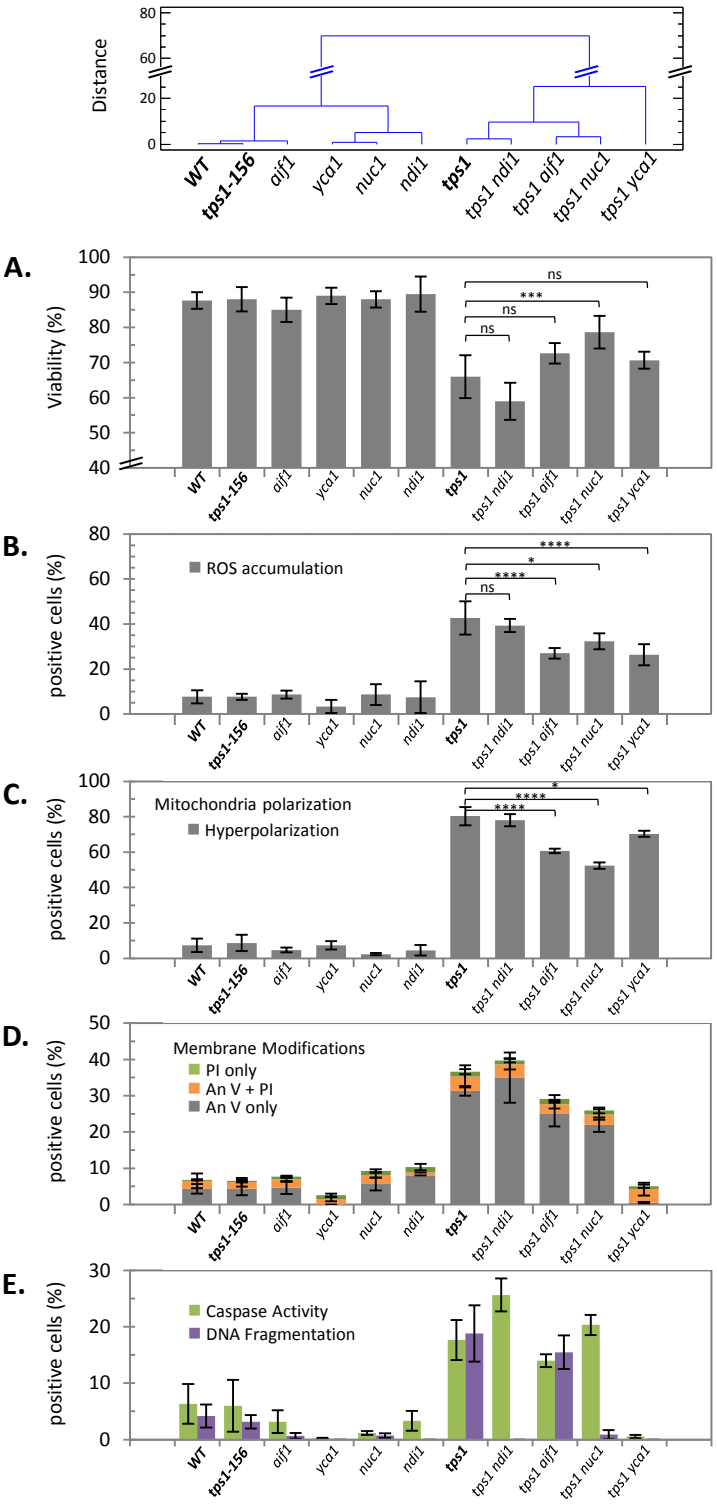
Distance
80
60
20
0
WT
tps1-156
aif1
yca1
nuc1
ndi1
tps1
tps1 ndi1
tps1 aif1
tps1 nuc1
tps1 yca1
A.
Viability (%)
100
90
80
70
60
50
40
ns
***
ns
ns
B.
positive cells (%)
ROS accumulation
****
*
****
ns
C.
positive cells (%)
Mitochondria polarization
Hyperpolarization
*
****
****
D.
positive cells (%)
Membrane Modifications
PI only
An V + PI
An V only
50
40
30
20
10
0
E.
positive cells (%)
Caspase Activity
DNA Fragmentation
30
20
10
0

Figure 5

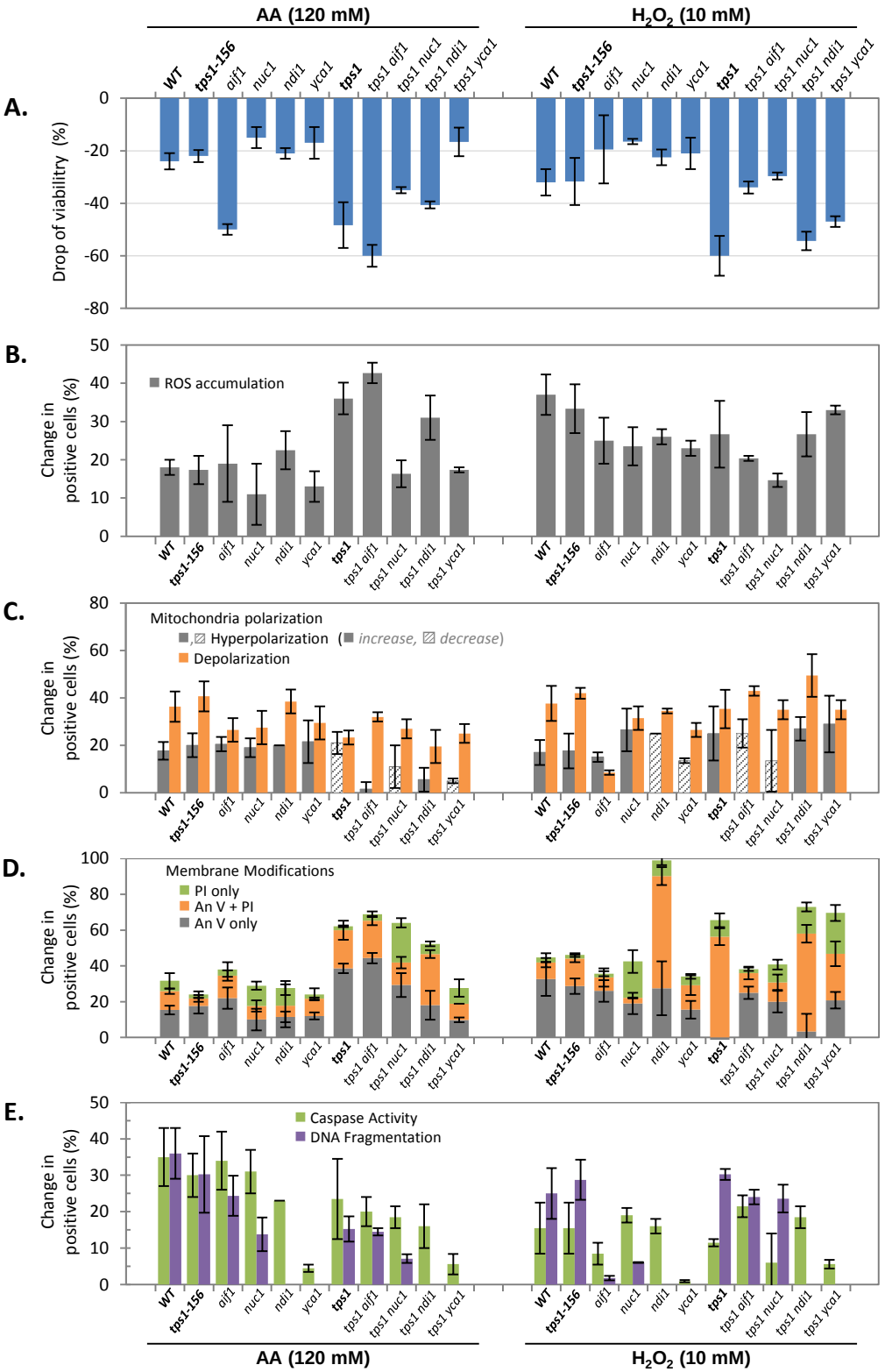
AA (120 mM)
H2O2 (10 mM)
WT
tps1-156
aif1
nuc1
ndi1
yca1
tps1
tps1 aif1
tps1 nuc1
tps1 ndi1
tps1 yca1
A.
Drop of viability (%)
B.
ROS accumulation
Change in positive cells (%)
C.
Mitochondria polarization
Hyperpolarization (increase, decrease)
Depolarization
D.
Membrane Modifications
PI only
An V + PI
An V only
E.
Caspase Activity
DNA Fragmentation

Figure 6

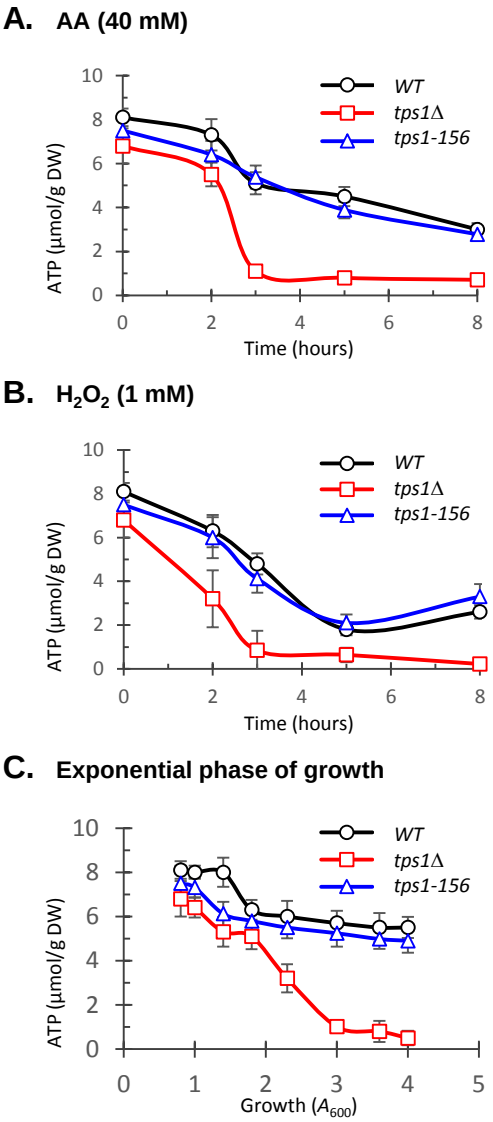
A. AA (40 mM)
WT
tps1Δ
tps1-156
ATP (µmol/g DW)
Time (hours)
B. H2O2 (1 mM)
WT
tps1Δ
tps1-156
ATP (µmol/g DW)
Time (hours)
C. Exponential phase of growth
WT
tps1Δ
tps1-156
ATP (µmol/g DW)
Growth (A600)

Figure S1

A.

Representative growth curve, (evolution of A_{600} as a function of time), (*or* total cell number as a function of time), with :

- t_0 : arbitrary origin of time (first sample taken during early log phase)
- t : time of sampling
- **N_t : Total cell number, (dead + viable cells),** determined by cytometry.
- **N_v : Viable (*i.e.* dividing) cells number** , evaluated by cytometry (Guava® ViaCount® Viability kit)

Each of these experimental growth curves, enables :

Direct calculation of :

- ✓ **μ**, the « *Apparent* » specific growth rate of cell population, from the fitting exponential curve
- ✓ **Viability***, *i.e.* the mean viability value observed during this specific culture

Indirect estimation (Panel C1 to C4) of :

- ✓ **μ_i**, the « *Intrinsic* » specific growth rate of dividing cells

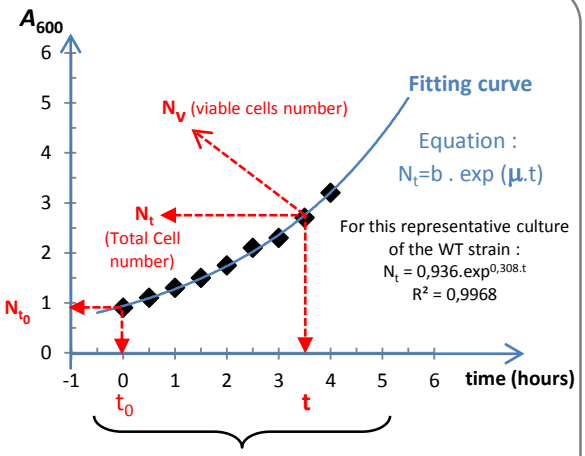

From all time-points during this exponential phase,

C.1.

Viable cells can **DIVIDE,** but some of them **DIE**

In a closed system (batch culture), if considering a quasi-stationary state (*i.e.* constant evolution rates μi & μd),

Evolution of viable cells:

(1) $dN_v = N_v \mu_i . dt - N_v \mu_d . dt$

Evolution of total number of cells ($dN_t = dN_v + dN_d$)

Considering (1) and $dN_d = N_v \mu_d . dt$:

(2) $dN_t = N_v \mu_i . dt$

- **N_t : Total** cell number, (dead + viable cells), at t
- **N_v :** Number of **Viable (*i.e.* dividing)** cells, at t
- **N_d :** Number of **dead** cells, at t
- μ_i : Growth rate of dividing cells (*i.e.* « *intrinsic* » growth rate)
- μ_d : Death rate

C.2.

Integral forms of equations (1) and (2) :

(3) $N_v = N_{v_0} . \exp [(\mu_i - \mu_d).t]$

(4) $N_t = N_{t_0} + N_{v_0}. [\mu_i /(\mu_i - \mu_d)] . (\exp [(\mu_i - \mu_d).t] -1)$

- N_{t_0} and N_{v_0} **:** total and viable cells, respectively, at t_0

C.3.

From these two, independant equations ((3) and (4)), we can solve the system and determine the two unknowns μ_i and μ_d by plotting :

(5) $\text{Ln} (N_v / N_{v_0}) = (\mu_i - \mu_d) . t$

(6) $(N_t - N_{t_0}) = [\mu_i /(\mu_i - \mu_d)] . (N_v - N_{v_0})$

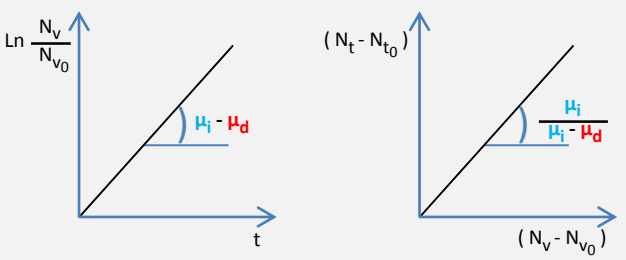

B.

μ (h^{-1}), « *Apparent* » specific growth rate of cell population

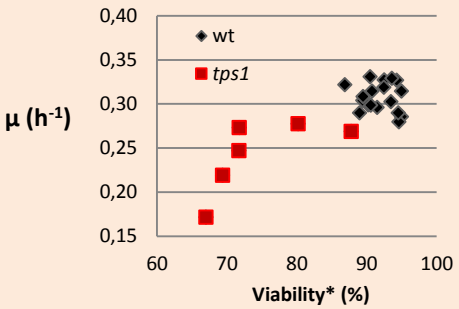

One point = one culture, as the one shown in panel A.

* Mean viability value during the culture

C.4.

μ_i (h^{-1}), « *Intrinsic* » specific growth rate of dividing cells

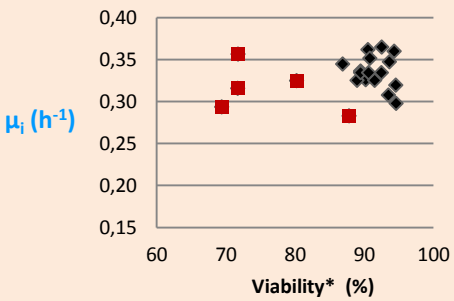

* Mean viability value during the culture

Figure S2

A. Exponentially growing strains (A_{600}~1)

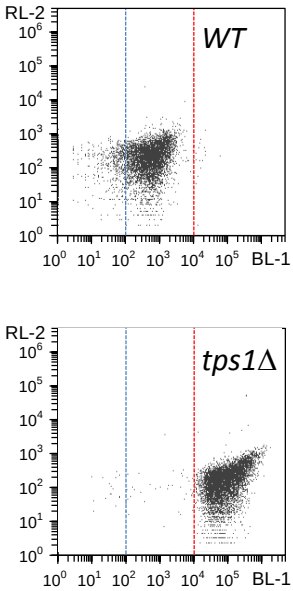

B. Control assays for depolarization or hyperpolarization, on WT cells

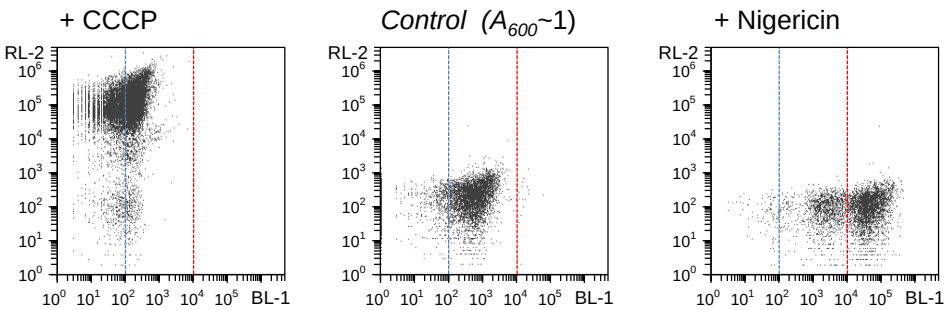

Figure S3

CEN.PK

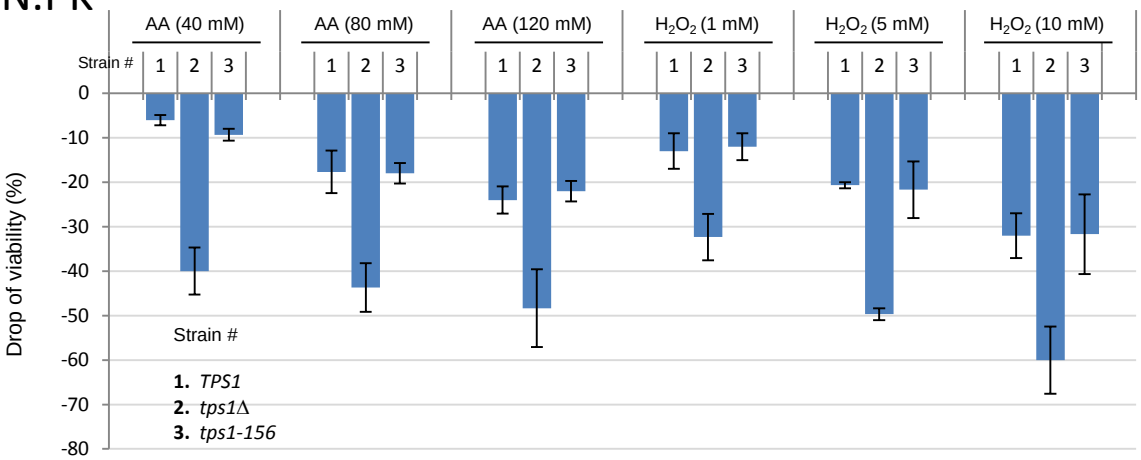

BY

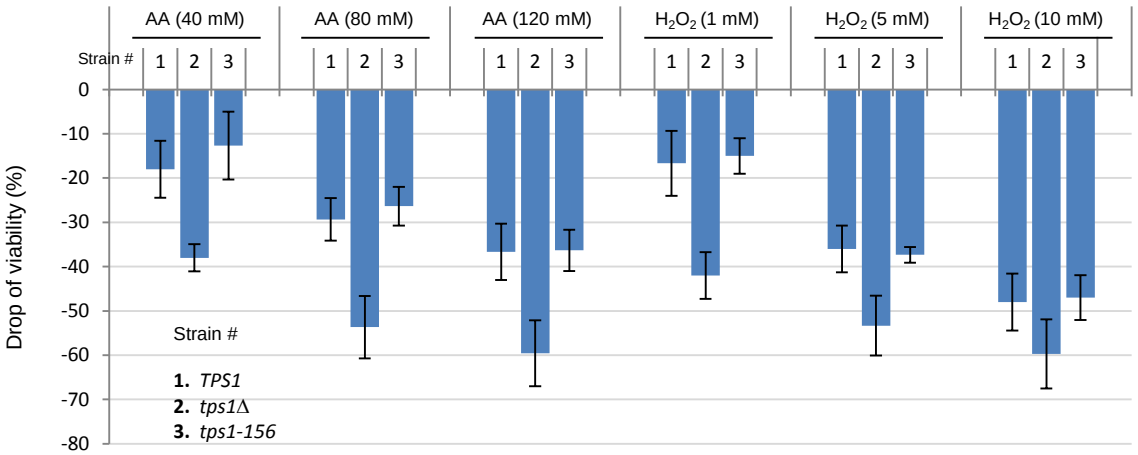

Click here to download Supplementary Material: Table S1 - Sup data to Fig.1 - Exponential phase.xlsx

Click here to download Supplementary Material: Table S3 - Sup data to Fig.3 -AA & Peroxide exposure.xlsx

Click here to download Supplementary Material: Table S5 - Sup data to Fig.5 -Stress exposure- double mutants.xlsx

Click here to download Supplementary Material: Table S4 - Sup data to Fig.4 -Exp phase- double mutants.xlsx

Click here to download Supplementary Material: Table S2 - Sup data to Fig.2 -CLS.xlsx